KINETICS OF ROULEAU FORMATION

II. Reversible Reactions

RICHARD W. SAMSEL
Division of Biology and Medicine, Brown University, Providence, Rhode Island 02912

ALAN S. PERELSON
Theoretical Division, University of California, Los Alamos National Laboratory, Los Alamos, New Mexico 87545

ABSTRACT Red blood cells aggregate face-to-face to form long, cylindrical, straight chains and sometimes branched structures called rouleaux. Here we extend a kinetic model developed by R. W. Samsel and A. S. Perelson (1982, *Biophys. J.* 37:493–514) to include both the formation and dissociation of rouleaux. We examine thermodynamic constraints on the rate constants of the model imposed by the principle of detailed balance. Incorporation of reverse reactions allows us to compute mean sizes of rouleaux and straight chain segments within rouleaux, as functions of time and at equilibrium. Using the Flory-Stockmayer method from polymer chemistry, we obtain a closed-form solution for the size distribution of straight chain segments within rouleaux at any point in the evolution of the reaction. The predictions of our theory compare favorably with data collected by D. Kernick, A.W.L. Jay, S. Rowlands, and L. Skibo (1973, *Can. J. Physiol. Pharmacol.* 51:690–699) on the kinetics of rouleau formation. When rouleaux grow large, they may contain rings or loops and take on the appearance of a network. We demonstrate the importance of including the kinetics of ring closure in the development of realistic models of rouleaux formation.

I. INTRODUCTION

Joseph Lister, the father of the modern theory of infectious disease, in a paper read before the Royal Society of London in 1857, noted that "if a drop of human blood just shed is placed between plates of glass and examined with a microscope, the red corpuscles are seen to become applied to one another by their flat surfaces, so as to form long cylindrical masses like piles of money ... [with] the terminal corpuscles of each 'rouleau' adhering to other rouleaux, a network is produced" (Lister, 1859). Although Lister and others correlated the presence of large, stable rouleaux with states of disease, it was not until seventy years later that the size distribution of rouleaux was examined quantitatively from a theoretical and an experimental point of view (Ponder, 1927). In the last two decades there has been a resurgence of interest in rouleaux, and recent work has served to elucidate the mechanism of rouleau formation (Brooks and Seaman, 1973; Brooks, 1973*a, b, c;* Chien, 1975, 1981; Skalak et al., 1981; Samsel and Perelson, 1982) and its physiological significance (Chien, 1975; Dintenfass, 1976). The kinetics of red cell aggregation has received relatively less attention until recently. Kernick et al. (1973) have reexamined Ponder's (1927) model; Mills et al (1980*a*) studied the kinetics of linear rouleau formation in a Couette flow by laser light backscatter; and Zaiko and Zaretskaja (1981) have predicted reaction rates for linear rouleaux in a shear field. However, each of these studies of kinetics has assumed rouleaux to be linear, cylindrical structures. In a vessel wider than the major diameter of a red cell, the branching of rouleaux is prominent (Goldstone et al., 1970), and we feel it to be an important determinant of their kinetic behavior (see Fig. 1).

Describing as a function of time the size of straight chain rouleaux and the branched structures they form, is the general kinetic problem of rouleau formation that we began attacking in our previous paper of this series (Samsel and Perelson, 1982). To simplify matters we restricted our attention in that paper to irreversible binding between red cells. Although at sufficiently short times after aggregation begins all adhesive interactions appear irreversible, it is known that under the influence of shear, red cells in rouleaux separate (Usami et al., 1975; Mills et al., 1980*b*). Adler (1979) has shown that stresses generated within an aggregate as it sediments can lead to disaggregation. Surface active agents and other chemical treatments (e.g., addition of streptokinase) can lead to the disaggregation of erythrocyte aggregates (Ehrly, 1971). Moreover, thermodynamics holds that all reactions are reversible and so

Reprint requests should be sent to Dr. Perelson.

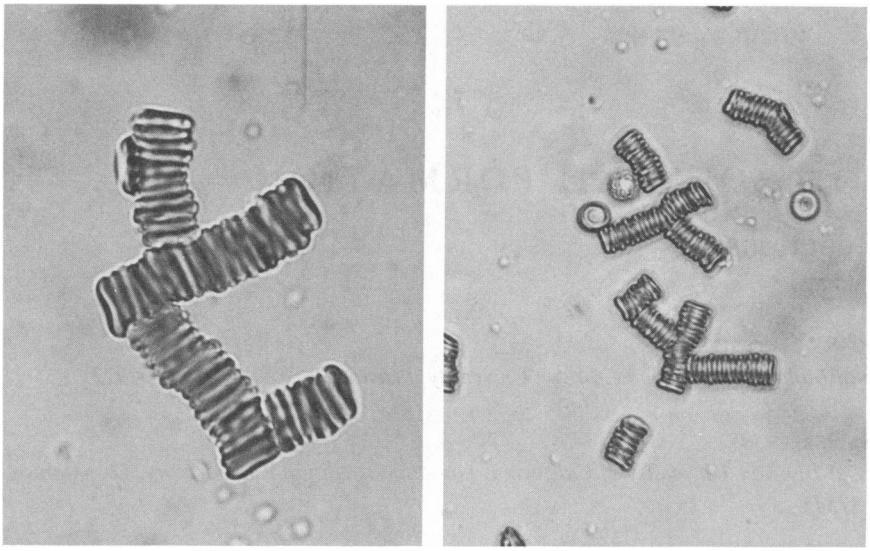

FIGURE 1 Branched rouleaux. Fresh blood from a healthy individual, anticoagulated with EDTA, was centrifuged and resuspended in its own plasma at a hematocrit of 1%. A drop of the resulting suspension was placed on a microscope slide, covered with a glass coverslip, and photographed with phase contrast and oil immersion optics. Placing the coverslip on the slide created the fluid motion driving red cell aggregation.

adhesions between red cells eventually must break, even in the absence of shear. Here we shall generalize our previous work and consider both the formation and breakup of rouleaux. Furthermore, we indicate the importance of including the formation of loops (cyclical rouleaux) in kinetic models designed to study the later phases of the aggregation process.

The kinetic model that we develop is based upon the law of mass action and is similar in many respects to those used in polymer chemistry. We describe the interactions between single red blood cells and rouleaux, and the interactions between rouleaux, by reversible mass-action reactions each characterized by a forward and reverse rate constant, k and k^r, respectively. By formulating the model in this way we are implicitly making assumptions about the physical processes leading to collisions between red cells and red cell aggregates and the physical processes responsible for the breakup of aggregates. As discussed in our previous paper (Samsel and Perelson, 1982), we assume that in any particular experiment the rate constants are "constants," whose value will depend on the physical conditions that characterize the experiment, e.g., the temperature, viscosity and density of the suspending medium, the concentration and type of bridging macromolecules, and other chemical constituents of the medium that affect cell-cell adhesion, and the hydrodynamic flows present in the experimental apparatus. For particles as large as red cells, diffusion is not an effective transport mechanism, and sedimentation and fluid motion are the predominant effects influencing particle collisions and aggregate dissociation. Although these forces are not isotropic, we shall assume that one can find appropriate average forward and reverse rate constants, which are the same at all positions within the volume, that to a fair degree of approximation characterize the experimental system. Sedimentation effects can in principle be eliminated by using a suspending media in which red cells are neutrally buoyant. Alternatively, studies of red cell aggregation and blood viscosity under near zero gravity may be carried out on the space shuttle (Dintenfass, 1979) with sedimentation effects eliminated. Fluid forces then determine the rate constants.

As another stage in the modeling process, which is beyond the scope of this paper, one can develop theoretical methods of choosing the rate constants appropriate to the hydrodynamic situation. Work in this direction has already begun. With regard to choosing forward rate constants, Jones and Perry (1979) and Saffman and Turner (1956) discuss aggregation in turbulent flow fields, while Capo et al. (1982), Zaiko and Zaretskaya (1981), Bell (1981), Evans and Proctor (1978), Chang and Robertson (1976), Richardson (1973), Swift and Freidlander (1964), and Levich (1962) discuss aggregation in uniform shear fields. If a suspension of cells is agitated in some regular way, shear rates may be estimated (cf. Capo et al., 1982) and theoretical results applied. When one plots mean rouleau size against shear rate, one finds that as shear rate increases, the curve first increases, reaches a maximum, and then decreases (cf. Chien, 1976). The initial increase occurs because low shear rates enhance collisions between red cells. As one increases the shear rate further, collisions are enhanced, but high shear rates disaggregate rouleaux, and eventually this effect predominates. Mills et al. (1980*a*) suggest an empirical relation between mean rouleau size and shear rate. Translating a shear rate into a set of forward and reverse rate constants is an unsolved problem. For our purposes we shall simply assume that in

the low shear rate regime, the forward and reverse rate constants are chosen in such a way that association processes dominate; whereas in the high shear regime we assume that the forward and reverse rate constants are chosen in such a way that dissociation processes dominate.

In section II we describe a reversible model for rouleau formation and show how the principle of detailed balance can be used to identify an interdependence among the governing parameters. In section III we obtain, under reasonable assumptions, analytic solutions for the size distribution of branches using the Flory-Stockmayer method developed in polymer chemistry. In section IV we examine the predictions of our model for realistic ranges of parameter values. A discussion of our results and of the importance of loop formation in the end stages of reaction is given in section V.

To both simplify and shorten the presentation we shall use the same notation as in our previous paper (Samsel and Perelson, 1982) and refer to equations from that paper. Equation I.7 will refer to Eq. 7 in our previous paper; whereas Eq. 7 will refer to an equation derived in this paper. For the purposes of this paper, a rouleau will be taken to be any cluster of red cells whose geometry may be described as an aggregate of linear stacks.

II. REVERSIBLE KINETICS OF ROULEAU FORMATION

Reverse Reaction Kinetics

As in our previous paper, we model a red cell as a flexible cylindrical disk of radius r and thickness h, with two faces each having surface area $e = \pi r^2$ and a wall with surface area $w = 2\pi rh$. Red cells adhere face-to-face to form cylindrical stacks. A stack increases in length when a cell adheres to a small elongation zone at its end. The elongation zone contains the face of the end cell and the portion of the wall of the rouleau within some critical distance of its end. The two elongation zones at the ends of a stack are called caps, since they resemble the cap on an object such as a fountain pen. The area of a cap, a_c, can be chosen such that the cap is simply the end of a stack (i.e., $a_c = e$) or it can be chosen such that the cap includes a true elongation zone (e.g., $a_c = e + w$). A branched rouleau is modeled as an aggregate of linear stacks called segments or branches connected at right angles. A particular rouleau can be described as having n cells, b branches, p branch points, and c caps. For rouleaux that have the topological form of a tree, i.e., have no loops, we showed (Eq. I.25)

$$b = c - 1 \quad \text{and} \quad p = c - 2. \tag{1}$$

Consequently, only two variables, n and c, are needed to describe treelike rouleaux. Throughout this paper we will restrict our attention to treelike rouleaux and use the terms treelike rouleau and rouleau synonymously. (In a later publication we will consider the formation of rouleaux containing loops).

If we let $R(n,c)$ and $S(n,c)$ denote the concentration of rouleaux and segments with n cells and c caps, respectively, then as shown in our first paper systems of differential equations can easily be constructed that describe the time rate of change of these variables during an irreversible aggregation process. The generalization to reversible processes is more complex. A rouleau with n cells and c caps is not a unique object; for example, each segment in it can take on a variety of lengths. From a segment of length one, the loss of a single cell causes the disappearance of the segment and the loss of a cap. However, the dissociation of a single cell from the end of a segment of length two, or greater, has neither of these effects. Thus c may or may not decrease when a cell dissociates from a rouleau with n cells and c caps. Therefore, it is not possible, using the state variables n and c, to describe uniquely the products formed when rouleaux break up (although one could in principle enumerate all possible rouleau structures and average over that ensemble). By contrast, a given segment with n cells and c caps is geometrically unique, so it is therefore possible to predict the products formed by dissociation. Thus with reversible interactions, one can formulate an exact set of differential equations for $S(n,c)$. As we show below, from $S(n,c)$ one can obtain information about the

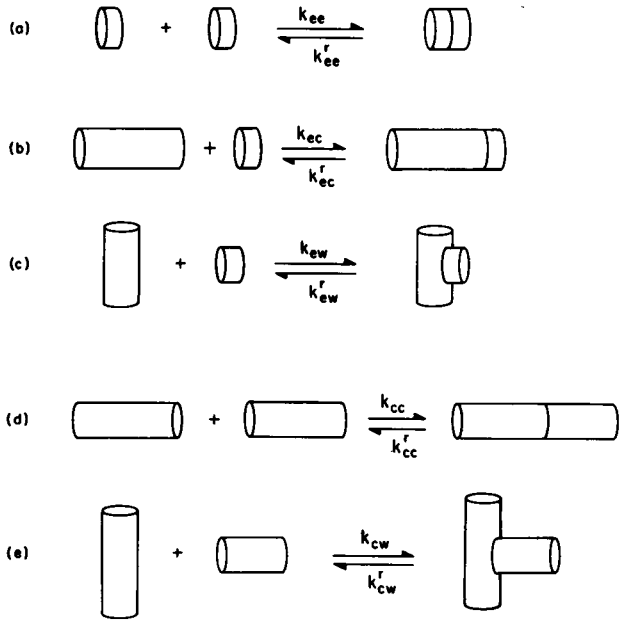

FIGURE 2 Diagrammatic representation of reactions that generate rouleaux. (*a*) Two erythrocytes react with rate constant per unit area k_{ee}. (*b*) An erythrocyte reacts with the cap on a rouleau with rate constant per unit area k_{ec}. This reaction elongates the rouleau. (*c*) An erythrocyte reacts with the wall of a rouleau to initiate a branch with rate constant k_{ew}. (*d*) Two rouleaux react via a cap-cap interaction with rate constant per unit area k_{cc}. (*e*) Two rouleaux react via a cap-wall interaction with rate constant k_{cw}. The reverse reactions and their rate constants are also shown.

mean rouleau size, degree of branching, and the total rouleau concentration.

In the formation of branched treelike rouleaux we assume that there are five reversible interactions as shown in Fig. 2. Two erythrocytes join face-to-face to form a two-cell rouleau with rate constant k_{ee} and dissociate with rate constant k^r_{ee}. A single erythrocyte can elongate a segment by joining face-to-face with the terminal cell or cap of the segment; k_{ec} and k^r_{ec} are the forward and reverse rate constant describing that process. Alternatively, a single red cell can initiate a branch by adhering to the wall of a segment with rate constant k_{ew}. A one cell segment can be eliminated by the dissociation of the single cell from the wall, with rate constant k^r_{ew}. Two segments can condense to form a longer segment by a cap-cap interaction with forward rate constant k_{cc}. Conversely, a long segment can break into two short segments, with rate constant k^r_{cc}. Via a cap-wall interaction two segments can condense and form a branched rouleau with forward rate constant k_{cw}, and a branched rouleau can break into straight segments by the reverse reaction with rate constant k^r_{cw}. The five reverse rate constants k^r_{ee}, k^r_{ec}, k^r_{ew}, k^r_{cc}, and k^r_{cw} all have units of time^{-1}, while the five forward rate constants are all given in units of volume area^{-1} time^{-1} as discussed in our previous paper.

The development of the set of differential equations for $S(n,c)$ describing reversible rouleau formation is presented in Appendix I. Here, we restrict our attention to deriving equations for the following overall descriptors of the aggregation process: E, the concentration of free erythrocytes; R, the total concentration of rouleaux; S, the total concentration of straight segments within rouleaux; M, the concentration of ends or "caps" on rouleaux; T, the concentration of external surface area on rouleaux; W, the concentration of "wall' area on the surface of rouleaux where branch initiation can occur; $\langle n\rangle_r$, the mean number of cells in a rouleau; $\langle n\rangle_s$, the mean number of cells in a segment; $\langle n\rangle_u$, the mean number of cells in a unit (i.e., a rouleau or free erythrocyte); $\langle n\rangle_{su}$, the mean number of cells in a straight chain unit (i.e., a rouleau segment or free erythrocyte); and $\langle b\rangle$, the mean number of "branches" or segments in a rouleau. The concentrations E, R, S, and M are all measured in units of number per unit volume; whereas the area concentrations T and W are measured in units of area per unit volume. One can show on the basis of conservation laws and geometric constraints that (see our previous paper)

$$\langle n\rangle_r = \frac{E_0 - E}{R}, \quad \langle n\rangle_s = \frac{E_0 - E}{S},$$

$$\cdot\ \langle n\rangle_u = \frac{E_0}{E + R}, \quad \langle n\rangle_{su} = \frac{E_0}{E + S}, \tag{2}$$

$$\langle b\rangle = S/R, \tag{3}$$

$$S = (1/2e)[(E_0 - E)w + (2e - a_c)M - W], \tag{4}$$

$$T = W + Ma_c, \tag{5}$$

and

$$R = M - S, \tag{6}$$

where E_0 is the total concentration of erythrocytes in the system and a_c is "reactive" surface area of a cap at which elongation of a segment can occur. (The interpretation of a_c is discussed in detail in our previous paper.)

Eq. 4–6 show that there are only three independent variables, E, M, and W, from which all the remaining variables may be found. Differential equations containing the terms contributed by the forward reactions were derived in our previous paper. Here we focus on the additional terms generated by the reverse reactions. In the differential equation for E the dissociation of a two-cell rouleau [i.e., $S(2, 2)$] contributes two free cells; the dissociation of a one-cell segment from a wall [i.e., $S(1, 1)$] contributes one free cell, as does the dissociation of a terminal cell on a segment containing one or two caps. Including the forward reaction terms from Eq. I.46 we have

$$dE/dt = -k_{ee}a_cE^2 - k_{ec}a_cME - k_{ew}EW + 2k^r_{ee}S(2,2) + k^r_{ew}S(1,1) + k^r_{cc}\sum_{c=0}^{2}\sum_{n=c+1}^{\infty} cS(n,c). \tag{7}$$

By a similar process, we modify Eq. I.47 for the cap concentration, M. Caps are created by the joining of erythrocytes with each other or with walls and are lost by the condensation of caps with each other or with walls. We add to these terms the loss of caps from dissociation of $S(1, 1)$ and $S(2, 2)$, as well as the gain of caps from the breakup of all branches. Not counted are terms resulting from the loss of single cells from caps other than $S(1, 1)$, since this process conserves the number of caps. Thus, we find

$$\begin{aligned} dM/dt = {} & k_{ee}a_cE^2 + k_{ew}EW - k_{cc}a_cM^2 - k_{cw}MW \\ & - 2k^r_{ee}S(2,2) - k^r_{ew}S(1,1) \\ & + 2k^r_{cc}\sum_{c=0}^{2}\sum_{n=c+1}^{\infty}(n - c - 1)S(n,c) \\ & + k^r_{cw}\sum_{c=0}^{2}\sum_{n=c+1}^{\infty}(2 - c)S(n,c). \end{aligned} \tag{8}$$

Finally, one can write an expression for the rate of change of the reactive wall area concentration W. We have the contributions from the association reactions (see Eq. I.49) in addition to contributions from each of the reverse reactions. Reactive wall area is lost when $S(1, 1)$ and $S(2, 2)$ dissociate and when single erythrocytes detach from caps. Moreover, the reactive wall area changes when branches break or dissociate from attached walls, with area factors identical but opposite in sign to those derived for

the association reactions. Thus we find

$$\begin{aligned} dW/dt = {} & (w - a_c + e)k_{ee}a_cE^2 + wk_{cc}a_cME \\ & + (w - a_c)k_{cw}EW + (a_c - e)k_{cc}a_cM^2 \\ & + (a_c - 2e)k_{cw}MW - 2(w - a_c + e)k^r_{ee}S(2,2) \\ & - (w - a_c)k^r_{cw}S(1,1) - wk^r_{cc}\sum_{c=0}^{2}\sum_{n=c+1}^{\infty} cS(n,c) \\ & - 2(a_c - e)k^r_{cc}\sum_{c=0}^{2}\sum_{n=c+1}^{\infty}(n - c - 1)S(n,c) \\ & - (a_c - 2e)k^r_{cw}\sum_{c=0}^{2}\sum_{n=c+1}^{\infty}(2 - c)S(n,c). \end{aligned} \quad (9)$$

Since each reverse reaction involves separating similar membrane areas, the energetics of the reactions ought to be similar. Under the assumption that the five rate constants for the reverse reactions are equal, one can evaluate the summations in Eqs. 7–9. If we define k_r so that

$$k_r \equiv k^r_{ee} = k^r_{cc} = k^r_{ew} = k^r_{cc} = k^r_{cw}, \quad (10)$$

then, using the facts that

$$S(n,c) = 0 \quad \text{if} \quad c > n,$$

$$\sum_{c=0}^{2}\sum_{n=c+1}^{\infty} cS(n,c) + S(1,1) + 2S(2,2) = M;$$

and

$$\sum_{c=0}^{2}\sum_{n=c+1}^{\infty} nS(n,c) + S(1,1) + 2S(2,2) + E = E_0,$$

it is easy to show that

$$dE/dt = -k_{ee}a_cE^2 - k_{cc}a_cME - k_{cw}EW + k_rM, \quad (11)$$

$$\begin{aligned} dM/dt = {} & k_{ee}a_cE^2 + k_{cw}EW - k_{cc}a_cM^2 \\ & - k_{cw}MW + 2k_r(E_0 - E) - 3k_rM, \end{aligned} \quad (12)$$

and

$$\begin{aligned} dW/dt = {} & (w - a_c + e)k_{ee}a_cE^2 + wk_{cc}a_cME \\ & + (w - a_c)k_{cw}EW + (a_c - e)k_{cc}a_cM^2 \\ & + (a_c - 2e)k_{cw}MW - 2k_r(a_c - e)(E_0 - E) \\ & - k_r(w - 3a_c + 4e)M + 2ek_rS. \end{aligned} \quad (13)$$

Replacing S by the expression involving E, M, and W from Eq. 4 we find

$$\begin{aligned} dW/dt = {} & (w - a_c + e)k_{ee}a_cE^2 + wk_{cc}a_cME \\ & + (w - a_c)k_{cw}EW + (a_c - e)k_{cc}a_cM^2 \\ & + (a_c - 2e)k_{cw}MW \\ & + k_r(w - 2a_c + 2e)(E_0 - E - M) - k_rW. \end{aligned} \quad (14)$$

While the reverse reaction terms in Eqs. 11–14 are surprisingly simple when compared with the corresponding terms in Eqs. 7–9, they do not seem to be intuitively transparent.

Equations for S and R may be determined from Eqs. 4 and 6 or may be derived directly from the detailed theory presented in Appendix I. The two approaches yield the same following result.

$$\begin{aligned} \frac{dS}{dt} = {} & \frac{1}{2}k_{ee}a_cE^2 + k_{cw}EW \\ & - \frac{1}{2}k_{cc}a_cM^2 + k_r(E_0 - E - M - S), \end{aligned} \quad (15)$$

$$\begin{aligned} \frac{dR}{dt} = {} & \frac{1}{2}k_{ee}a_cE^2 - \frac{1}{2}k_{cc}a_cM^2 \\ & - k_{cw}MW + k_r(E_0 - E - M - R). \end{aligned} \quad (16)$$

Eqs. 11–16 describe a general reversible kinetic model for rouleau formation. By making particular choices for the rate constants and parameters, different situations can be modeled. For example, if $k_{cc} = k_{cw} = k^r_{cc} = k^r_{cw} = 0$, then only reactions involving free erythrocytes occur with nonzero rate, and the model is thus reduced to a reversible addition polymerization model. (See our previous paper for a discussion of irreversible addition polymerization models). If condensation reactions are allowed, but $k_{cw} = k_{cc}$, $k^r_{cc} = k^r_{cw}$, and $a_c = e$, then no distinction is made between caps and walls, and the two rouleaux will adhere with equal probability at any place on their surfaces. Such a situation occurs at very high adhesive energies, the typical linear geometry of rouleau is lost, and the cells form clumps. To the extent that such clumps can be approximated by treelike aggregates, our theory should predict their size distribution.

RATE CONSTANT CONSTRAINTS

By using the principle of detailed balance (Bak, 1963; Katchalsky and Curran, 1965), one can show that the rate

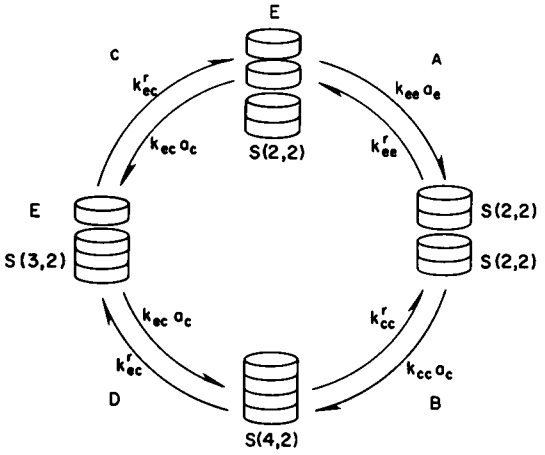

FIGURE 3 Two independent ways of generating a cylindrical rouleau containing four cells are indicated. Two erythrocytes can combine to form S (2,2) as indicated in reaction A. Two such dimers can then combine (reaction B). Alternatively, an erythrocyte can add to an already existent dimer (reaction C) to form the trimer, S (3,2). Another erythrocyte can then add to the trimer (reaction D) to form the four-cell rouleau S (4,2).

constants in Eqs. 11–16 are not all independent. Physically there are three independent processes in rouleau formation: initiation (by dimer formation), elongation, and branching. Consequently, one might suspect that there are only three independent equilibrium constants. In the equilibrium theory of rouleau formation of Perelson and Wiegel (1982) and Wiegel and Perelson (1982) initiation was not distinguished from elongation and the theory involved only two equilibrium constants. To obtain the appropriate constraints on the rate constants, consider the sequence of reactions shown in Fig. 3 in which a straight segment containing four cells and two caps is built by one of two pathways. Following the pathway on the right, involving the reactions labeled A and B, one finds that at equilibrium

$$\bar{S}(4,2) = \frac{k_{cc}a_c}{k^r_{cc}}\bar{S}(2,2)^2, \qquad \bar{S}(2,2) = \frac{k_{ee}a_e}{k^r_{ee}}\bar{E}^2,$$

where the overbars denote equilibrium concentrations. Following the pathway on the left, involving reactions C and D, one finds at equilibrium

$$\bar{S}(4,2) = \frac{k_{ec}a_c}{k^r_{ec}}\bar{S}(3,2)\bar{E}, \qquad \bar{S}(3,2) = \frac{k_{ec}a_c}{k^r_{ec}}\bar{S}(2,2)\bar{E}.$$

Thermodynamics demands that these equations be consistent.

Solving for $\bar{S}(4,2)$ in terms of $\bar{E}$ gives two alternate expressions that when equated yield the following constraint

$$\frac{k_{cc}a_c k_{ee}a_e}{k^r_{cc}k^r_{ee}} = \left(\frac{k_{ec}a_c}{k^r_{ec}}\right)^2 \tag{17}$$

If all the reverse rate constants are equal as in Eq. 10, then this reduces to

$$k_{cc} = \frac{k^2_{ec}a_c}{k_{ee}a_e}. \tag{18}$$

The generation of a cylindrical rouleau of any size must involve initiation and elongation by either cap-cap or erythrocyte cap reactions (the processes depicted in Fig. 3). Analyzing additional nonbranched states, which can be reached by multiple pathways, involves further concatenation of these processes but does not yield any additional constraints.

Fig. 4 illustrates a branched rouleau that can be obtained by two independent kinetic pathways. We obtain an additional constraint on the rate constants by application of the technique illustrated above. Analyzing the equilibrium concentrations of any of the species in the cycle shows that

$$\frac{k_{ew}k_{ec}a_c}{k^r_{ew}k^r_{ec}} = \frac{k_{cw}k_{ee}a_e}{k^r_{cw}k^r_{ee}}. \tag{19}$$

These constraints may also be found using the Wegscheider relations (Bak, 1963), which state that the product of the rate constants following the cycle in the clockwise direction equals the product of the rate constants obtained by following the cycle in the counter-clockwise direction. Under the assumption of equal reverse rate constants, Eq. 19 reduces to

$$k_{cw} = \frac{k_{ew}k_{ec}a_c}{k_{ee}a_e}. \tag{20}$$

Since branching must occur by the addition of a single cell or a longer segment, analyzing other branched states that can be reached by multiple pathways does not yield any new constraints.

There is one additional constraint that we may impose on the rate constants that will further simplify our analysis. If we view an erythrocyte as a segment of length one with two caps, then either of these caps could attach to the end of a growing segment in a typical cap-cap reaction. Hence it seems reasonable to assume

$$k_{ec} = 2k_{cc}, \tag{21}$$

in which case initiation is no longer distinguished from elongation. As a consequence, we may define a single forward rate constant per unit area for all cap-cap reactions,

$$k_c \equiv k_{cc} = k_{ec}/2. \tag{22}$$

Using detailed balance, Eq. 18, one obtains the additional

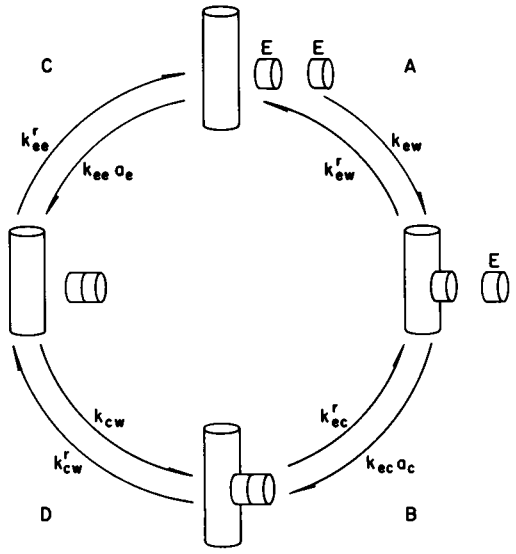

FIGURE 4 Two independent ways of forming a branched rouleau containing a cylindrical stack and a two-cell branch are indicated. An erythrocyte can attach to the wall of an existent rouleau by an erythrocyte-wall reaction (reaction A), and then via an erythrocyte-cap reaction (reaction B) the branch can elongate. Alternatively, the two erythrocytes can first combine via an erythrocyte-erythrocyte reaction (reaction C) and then the dimer can attach to the wall of an existent rouleau by a cap-wall reaction (reaction D).

identity

$$k_c = k_{ee}a_e/4a_c. \tag{23}$$

Substituting Eqs. 22 and 23 into Eq. 20 allows us to define a single forward rate constant per unit area for cap-wall reactions

$$k_w \equiv k_{cw} = k_{ew}/2. \tag{24}$$

Thus the two rate constants, k_c and k_w, can be used to characterize all the forward reactions shown in Fig. 1.

III. AN EXACT SOLUTION FOR THE SIZE DISTRIBUTION OF SEGMENTS

Flory-Stockmayer Method

A statistical method developed in polymer chemistry to find the molecular weight distribution of the products of a condensation polymerization reaction (cf. Flory, 1953; Stockmayer, 1943; Perelson, 1980), may be used to determine the size distribution of straight chain segments in rouleaux. In Appendix I we use the model outlined in section II to derive a set of differential equations for $S(n,c)$, the concentration of segments with n cells and c caps. Assuming that the aggregation process begins with monodisperse erythrocytes, we can immediately obtain a solution to these differential equations via the Flory-Stockmayer statistical method. This solution is then verified by direct substitution into the equations given in Appendix I.

Following Flory (1953) we view each face of an erythrocyte as a "reactive site." Reactive sites may be bound together, bound to a wall, or free. The two basic assumptions underlying the Flory-Stockmayer method are that every free site be equally reactive, irrespective of the size and shape of the aggregate on which it is found, and that aggregates grow in a treelike fashion (i.e., without forming loops). To develop a model consistent with the hypothesis of equal reactivity, we need to assume that sites on erythrocytes are equivalent to sites on the end of a branch. Hence we can not distinguish between initiation and elongation, nor between erythrocyte-wall and cap-wall reactions. Consequently, to use the Flory-Stockmayer method we must assume that there are only two forward rate constants, k_c and k_w, characterizing rouleau formation. Although the method is probably consistent with two separate reverse rate constants, "k_c^r and k_w^r," we have restricted our investigations to the case of only one reverse rate constant k_r.

Denote by p_f the fraction of the reactive sites that are free. For systems containing an infinite number of particles, p_f is the probability that a randomly chosen reactive site is free. Here we assume that the total number of red cells in the system is large enough for this interpretation to be valid. (The use of ordinary differential equations to describe the dynamics of aggregation is based on a similar assumption about the number of red cells in the system). To determine p_f, notice that the concentration of free sites is equal to the concentration of caps plus twice the concentration of free erythrocytes. The total concentration of reactive sites, free or bound, is twice the total concentration of erythrocytes. Hence

$$p_f = \frac{2E + M}{2E_0}. \tag{25}$$

Similarly, the probability, p_w that a reactive site is bound to a wall is the ratio of the concentration of branch points to the total concentration of sites. Since the end of a segment is either a branch point or a cap, the concentration of branch points is $2S - M$. Thus

$$p_w = \frac{2S - M}{2E_0}. \tag{26}$$

The concentration of reactive sites bound to other sites is the total concentration of bound sites, $2(E_0 - E)$, minus the concentration of sites in caps or branch points, $2S$. Consequently, p, the probability that a site is bound to another site is given by

$$p = \frac{E_0 - E - S}{E_0}. \tag{27}$$

Because a site is either free, bound to a wall, or bound to another site

$$p_f + p_w + p = 1. \tag{28}$$

To compute $S(n,c)$ select a free site at random. The probability that it is part of an n-cell, two-cap segment is $p^{n-1}\,p_f$, the probability that $n - 1$ successive sites are bound to other sites, followed by one site that is free. In a unit volume, there are $2E + M$ free sites that can be chosen as the random free site. Choosing each one once will double count the number of segments with two caps since each of the two caps on the segment will have been chosen once. Hence the number of segments with n cells and two caps per unit volume is given by $S(n,2) = (2E + M)p^{n-1}\,p_f/2$, $n = 2, 3, \ldots$. Using the definition of p_f, we find

$$S(n,2) = E_0 p_f^2 p^{n-1},\ n = 2, 3, \ldots. \tag{29}$$

In a like manner we can find the concentrations $S(n,1)$ and $S(n,0)$. Starting with a free site, the probability of finding $n - 1$ sites bound to other sites, followed by a site bound to a wall, is $p^{n-1}\,p_w$. Since there is only one free site per segment, $S(n,1) = (2E + M)p^{n-1}p_w$, $n = 1, 2, \ldots$., which can be rewritten as

$$S(n,1) = 2E_0 p_f p_w p^{n-1},\ n = 1, 2, \ldots. \tag{30}$$

Similar reasoning, but now starting at a bound site, leads to

$$S(n,0) = E_0 p_w^2 p^{n-1},\ n = 1, 2, \ldots. \tag{31}$$

Let $S_T(n)$ be the total concentration of segments of length n, irrespective of the number of caps. Then it is easy to show that

$$S_T(n) \equiv \sum_{c=0}^{2} S(n,c) = E_0(1-p)^2 p^{n-1}, \; n = 2, 3, \ldots . \quad (32a)$$

The case $n = 1$ is special since by definition a rouleau must contain at least two cells. A unit with two caps and one cell is a free erythrocyte and is not considered to be a segment in a rouleau. The only one-cell segments must be attached to a wall of another segment. Thus

$$S_T(1) \equiv S(1,0) + S(1,1) = E_0 p_w (p_w + 2p_f) \quad (32b)$$

Rather than measuring the concentrations $S(n,c)$ or $S_T(n)$, an easier experimental test of the theory would be to examine the concentration of segments with zero-, one-, or two-free caps, and any number of cells. Thus, we define

$$S(0) = \sum_{n=1}^{\infty} S(n,0), \qquad S(1) = \sum_{n=1}^{\infty} S(n,1),$$

and

$$S(2) = \sum_{n=2}^{\infty} S(n,2). \quad (33)$$

These segment concentrations are related to the macroscopic parameters, M and S, by the obvious relations

$$S = S(0) + S(1) + S(2) \quad (34)$$

and

$$M = 2S(2) + S(1). \quad (35)$$

Since $M = R + S$,

$$R = S(2) - S(0). \quad (36)$$

In the "site model" described above, $S(n,0)$, $S(n,1)$, and $S(n,2)$ are given explicitly by Eqs. 29–31. Substituting these equations into Eq. 33, we can immediately perform the summations and obtain

$$S(0) = \frac{E_0 p_w^2}{1-p}, \qquad S(1) = \frac{2E_0 p_f p_w}{1-p},$$

and

$$S(2) = \frac{E_0 p_f^2 p}{1-p}. \quad (37)$$

Thus

$$S = E_0(p_f + p_w - p_f^2), \quad (38)$$

$$M = 2E_0 p_f (1 - p_f), \quad (39)$$

and

$$R = E_0(p_f - p_w - p_f^2). \quad (40)$$

We may obtain E from Eqs. 27, 28, and 38 or by identifying an erythrocyte as a segment with one cell and two caps and using Eq. 29. Either approach gives

$$E = E_0 p_f^2. \quad (41)$$

Combining Eqs. 4, 38, 39, and 41 gives

$$W = E_0[w(1 - p_f^2) - 2a_c p_f(1 - p_f) + 2e(p_f - p_w - p_f^2)]. \quad (42)$$

Finally, using Eqs. 2 and 3 along with Eqs. 38–41, we can find various mean quantities that describe rouleau size and shape. For example, the mean rouleau size

$$\langle n \rangle_r = \frac{1 - p_f^2}{p_f - p_w - p_f^2}. \quad (43)$$

The other mean quantities (Eqs. 2 and 3) are as easily found.

The probabilities p, p_w, and p_f given by Eqs. 25–27 depend on time, as do E, M, and S. However, at any given time, as well as after the system has attained equilibrium, p, p_w, and p_f are simply constants and the size distribution of segments is given by Eqs. 29–31. By differentiating Eqs. 25–27, and substituting into the resulting expressions, Eqs. 11, 12, 14–16, 21–24, and 38–42, one can prove that the time evolution of p_f and p_w is governed by the pair of differential equations

$$\frac{dp_f}{dt} = -k_w E_0(2a_c - 2e - w)p_f^3 + 2E_0[k_w(a_c - e) - k_c a_c]p_f^2 - (k_w E_0 w + k_r)p_f + 2ek_w E_0 p_f p_w + k_r \quad (44a)$$

$$\frac{dp_w}{dt} = k_w E_0(2a_c - 2e - w)p_f^3 - 2k_w E_0(a_c - e)p_f^2 + wk_w E_0 p_f - 2ek_w E_0 p_f p_w - k_r p_w, \quad (44b)$$

and p may be determined from

$$p(t) = 1 - p_f(t) - p_w(t). \quad (44c)$$

Using these equations and the chain rule for differentiation of products of functions, one can directly verify that the segment size distribution obtained above solves the differential equations for $S(n,c)$ derived in Appendix I, Eqs. A1.1–A1.5, with rate constants chosen according to Eqs. 10, 21–24. A useful strategem for doing verifications of this type is discussed in DeLisi and Perelson (1976).

It should be obvious that this statistical method does not yield solutions to differential Eqs. A1.1–A1.5 for all choices of initial conditions and rate constants. Clearly, the initial conditions for $S(n,c)$ need to agree with those that are chosen for E, M, and S in Eqs. 11, 12, and 15, and need to be consistent with the distribution of segment sizes given by Eqs. 29–31. This is the case for the initial condition of

interest here, i.e., monodisperse red cells. Further, the same rate constants need to be chosen in Eqs. A1.1–A1.5 for $S(n,c)$ as in Eqs. 11, 12, and 15, and these rate constants must be consistent with the notion that all sites are equally reactive with respect to cap-cap and cap-wall reactions. This latter constraint motivated our use of a single cap-cap forward rate constant, k_c, and a single cap-wall forward rate constant, k_w, as defined by Eqs. 22–24.

IV. NUMERICAL EVALUATIONS

Nondimensionalization

By numerically solving Eq. 44, we can determine the probabilities p, p_f, and p_w as functions of time and then extract dynamical information about rouleau sizes and shapes from Eqs. 29–31, 38–43, and 2–3. As long as $k_r \neq 0$, the equilibrium values of p, p_f, and p_w may be found by setting the time derivatives to zero in Eq. 44 and solving the resulting system of nonlinear algebraic equations. An analytic solution to the equilibrium problem may be found in this way, but the resulting formulas are so complicated that we have not found them to be particularly helpful.

The site model has four independent parameters, k_c, k_w, k_r, and the hematocrit reflected in the initial red cell concentration E_0. To reduce the number of parameters even further, we reformulate Eq. 44 in terms of dimensionless quantities. To do so, we choose a reference time scale, τ, and a reference area, A. A nondimensional form of Eqs. 44a and 44b can now be written as follows

$$\frac{dp_f}{dt'} = -k'_w\left(\frac{2a_c - 2e - w}{A}\right)p_f^3 + 2\left[k'_w\left(\frac{a_c - e}{A}\right) - k'_c\right]p_f^2 - \left[k'_w\frac{w}{A} + k'_r\right]p_f + 2k'_w\left(\frac{e}{A}\right)p_f p_w + k'_r, \quad (45a)$$

$$\frac{dp_w}{dt'} = k'_w\left(\frac{2a_c - 2e - w}{A}\right)p_f^3 - 2k'_w\left(\frac{a_c - e}{A}\right)p_f^2 + k'_w\left(\frac{w}{A}\right)p_f - 2k'_w\left(\frac{e}{A}\right)p_f p_w - k'_r p_w, \quad (45b)$$

where $t' = t/\tau$, $k'_w = k_w A E_0 \tau$, $k'_c = k_c a_c E_0 \tau$, and $k'_r = k_r \tau$ are dimensionless quantities.

The choice of a reference time, τ, and a reference area, A, are to some degree arbitrary. The form of k'_w suggests that a reasonable choice for a reference area is $A = w$. Analogously, the forms of the three nondimensional-rate parameters suggest that there exist three reasonable choices for τ: $\tau_b = (k_w w E_0)^{-1}$, $\tau_e = (k_c a_c E_0)^{-1}$, and $\tau_d = k_r^{-1}$, which correspond to the characteristic times for branching, chain elongation, and dissociation. The choice of a reference time depends on which process one wishes to study. During the early stages of rouleaux formation, one expects chain elongation to be the dominant growth process. Therefore τ_e would be a good choice for τ. With this choice one finds

$$t' = k_c a_c E_0 t, \qquad k'_w = k_w w / k_c a_c, \qquad k'_r = k_r / k_c a_c E_0, \qquad \text{and } k'_c = 1. \quad (46)$$

Previously [see Eq. I.A4.1], we nondimensionalized rate constants by dividing them by $k_{ee}a_e$. However, by Eq. 23, $k_{ee}a_e = 4k_c a_c$. This factor of four should be kept in mind if one compares the simulations in this paper with those in our previous paper.

At longer times, branch formation is important, and choosing $\tau = (k_w w E_0)^{-1}$ would provide a time scale over which substantial branching would occur. In situations in which large rouleaux form, dissociation must be the slowest process, and the process that determines the time to reach equilibrium. (Equilibrium can only be approached after red cells have had enough time to associate and dissociate a few times.) When choosing $\tau = k_r^{-1}$ in order to study equilibrium processes, one finds

$$t' = k_r t, \qquad k'_r = 1, \; k'_w = k_w w E_0 / k_r,$$

and

$$k'_c = k_c a_c E_0 / k_r. \quad (47)$$

Notice that with this choice of τ, k'_w, and k'_c are nondimensional equilibrium constants characterizing branching and elongation.

In conducting numerical studies, it is also useful to use nondimensional quantities to characterize the concentrations of the various species. From Eqs. 38–42 one sees that it is natural to nondimensionalize all concentrations except W by dividing by E_0. Thus, for example, $S'(n,c) = S(n,c)/E_0$ and $R' = R/E_0$. The wall-area concentration is nondimensionalized by dividing by wE_0, i.e., $W' = W/wE_0$.

For our numerical evaluations we use the parameter values discussed in our previous paper. Thus we assume the area of cap, $a_c = e + w$. The geometric factors in our nondimensional equations can be computed once the ratio, h/r, of the height to the radius of the red cell is specified. From measurements on human erythrocytes given by Evans and Fung (1972) we concluded in our previous paper that $h/r = 0.62$. The initial concentration of erythrocytes, E_0, depends on the hematocrit (*hct*). The hematocrit, or volume concentration of red cells, is the most commonly used experimental measure of red cell density. A 1% hematocrit corresponds to $\sim 10^8$ erythrocytes/cm^3 (Miale, 1977); thus we take $E_0 = hct \times 10^8$ erythrocytes/cm^3, where *hct* is expressed as a number between 0 and 100. Normal human venous blood has a hematocrit of ~45%, and rouleau formation experiments are typically performed at hematocrits between 0.5% and 45%.

Kinetic Studies

We begin our numerical evaluations with a study of the kinetics of rouleau formation. Here we use the elongation time, $\tau_c = (k_c a_c E_0)^{-1}$, as a reference scale, so that Eq. 46 defines the nondimensional rate constants. To estimate k'_w we need to compare k_w, the rate constant for binding to a wall, with k_c, the rate constant for binding to a cap. Generally, a red cell cannot adhere as well to the side of a cylindrical rouleau as to its end; with equal membrane deformations being unable to bring as much surface area into direct contact with the curved side of the cylinder as with its somewhat flattened end. In our previous paper, our numerical results gave the most realistic predictions when $k_w \simeq 0.05\ k_c$. Here we will again assume $k_w \ll k_c$, or equivalently that $k'_w \ll 1$.

The parameter of most interest to this study is k_r, the rate constant characterizing the breakup of red cell adhesions. If $k_r = 0$, all reactions are irreversible; this is the case studied in our previous paper. For $k_r > 0$, the relevant parameter is k'_r, the ratio of the reverse rate constant to the constant characterizing the rate at which chain elongation occurs. When $k'_r \ll 1$ reactions are dominated by adhesion, large rouleaux should form. When $k'_r \simeq 1$, adhesion and dissociation are approximately balanced, whereas when $k'_r > 1$, dissociation dominates and small rouleaux form.

Fig. 5 shows how several of the variables in our theory change with time for differing values of k'_r with $k'_w = 0.1$

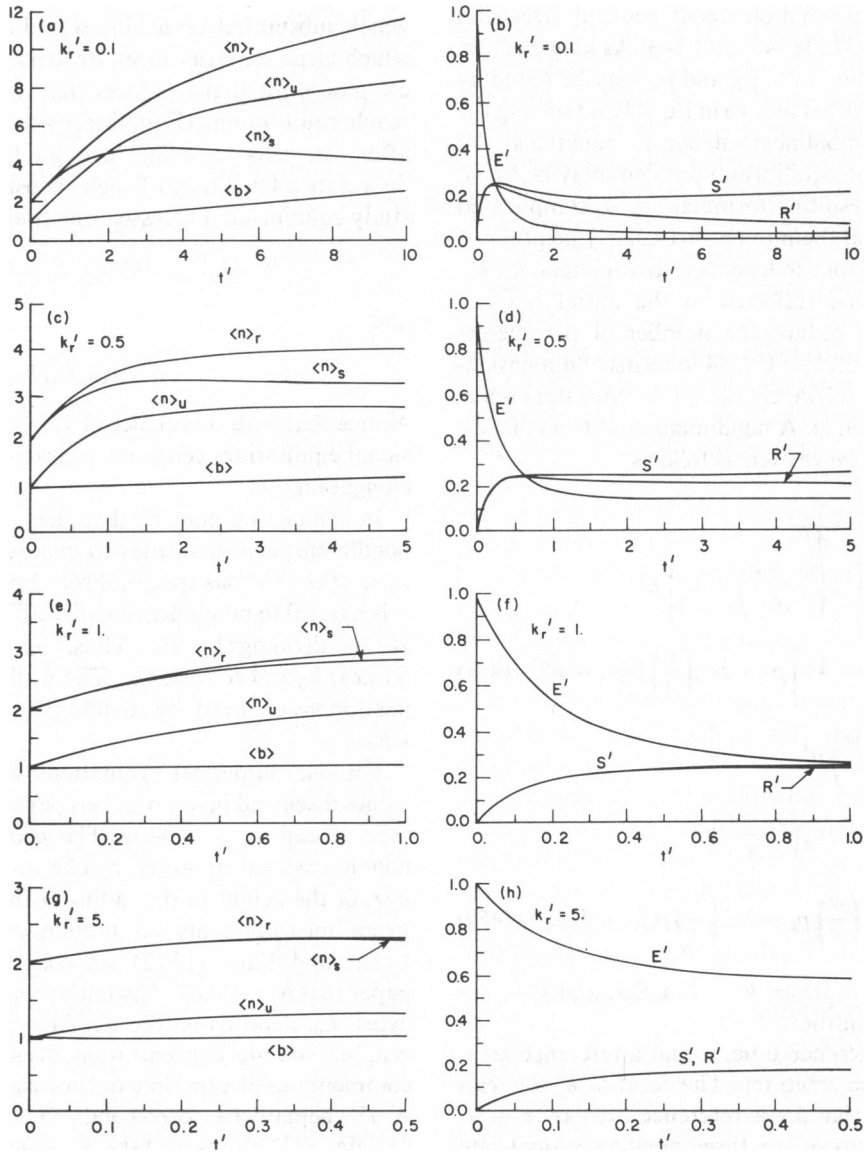

FIGURE 5 Dynamics of reversible rouleau formation at 1% hematocrit with $k'_w = 0.1$, for $k'_r = 0.1$, 0.5, 1.0, and 5.0. The mean rouleau size $\langle n \rangle_r$, the mean segment size, $\langle n \rangle_s$, the unit size $\langle n \rangle_u$, and number of branches per rouleau $\langle b \rangle$, are plotted vs. t' in the left panels. The nondimensional concentrations E', S', and R' are plotted vs. nondimensional time $t' = k_c a_c E_0 t$ in the right panels.

and $hct = 1$. The panels on the left show that the mean size of a rouleau, $\langle n \rangle_r$, constantly increases with times, as does the mean size of a unit, $\langle n \rangle_u$, and the mean number of branches, $\langle b \rangle$. The mean size of a segment, $\langle n \rangle_s$, does not always increase, as we now explain. The first rouleaux to appear are two cell aggregates. Thus $\langle n \rangle_r = \langle n \rangle_s = 2$ near $t = 0$. As time increases, rouleaux first grow as straight chains (see our paper) and thus $\langle n \rangle_s$ increases. As the rouleaux grow longer, branching becomes more probable. The growth of branches off straight segments then leads to a decrease in $\langle n \rangle_s$. This effect can be seen in Figs. 5 *a* and *c*. When $k_r' \geq 1$, large rouleaux do not form, branching is negligible, and hence $\langle n \rangle_s$ never decreases, as in Figs. 5 *e* and 5 *g*. Observe the panels on the right of Fig. 5. The concentration of free erythrocytes decreases rapidly and approaches a nonzero equilibrium value for all values of k_r'. The total concentration of rouleaux, R', initially increases as rouleaux are formed. When $k_r' < 1$, R' then decreases as small rouleaux combine into large ones (Fig. 5 *b*). Each rouleau is composed of one or more straight segments. Thus $S' \geq R'$. Large rouleaux tend to be branched and thus $S' < R'$ for small values of k_r' (Figs. 5 *b* and *d*). However, when k_r' is large, the mean size of a rouleau tends to two cells, and S' tends to R' (Figs. 5 *f* and *h*).

Kernick et al. (1973) studied the kinetics of rouleau formation of human erythrocytes. They showed that with blood from healthy individuals, either fresh or stored for various times and at various temperatures, diluted 100-fold in plasma, the mean unit length, $\langle n \rangle_u$, increases with time, starting from a value of one and saturating at a maximum value typically between two and three. (Note that Kernick et al. [1973] call $\langle n \rangle_u$ the mean rouleau length, not the mean unit size as we do.) As we demonstrated in our previous paper, irreversible models of rouleau formation never show this behavior. Instead, they invariably imply that $\langle n \rangle_u$ increases monotonically with time, never reaching a maximum value. By including reverse reactions we can now match the kinetic curves reported by Kernick et al. (1973). To illustrate this, in Fig. 6 we compare our theory with data from Kernick et al. (1973) on rouleau formation using freshly drawn blood from a healthy individual diluted to a hematocrit of 0.5%. For the parameter values used to generate Fig. 6 ($k_r' = 0.4$ and $k_w' = 0.2$), our theory predicted that $\langle b \rangle$ varied between 1.0 and 1.2, thus agreeing with the observation of Kernick et al. (1973) that under their experimental conditions rouleaux were linear.

Equilibrium Studies

One can estimate the time required for a system to approach equilibrium from the reciprocal of the rate constant describing the slowest process. In experiments where dissociation of rouleaux is allowed to occur spontaneously, rather than being driven say by high shear rates, we expect dissociation to occur slower than association, and consequently, we expect $1/k_r'$ to provide an estimate of the

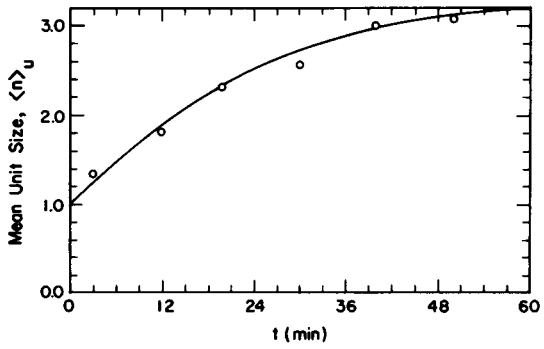

FIGURE 6 A comparison of the predicted time dependent growth of the mean unit size, $\langle n \rangle_u$, with data published by Kernick et al. (1973) on rouleaux formation using freshly drawn blood from a healthy individual. In both the experiment and theory, the hematocrit was 0.5%. To match the data, we chose $k_r' = 0.4$, $k_w' = 0.2$, and $t' = t/24$.

nondimensional time, t', required to approach equilibrium. (Analogously, $1/k_r$ provides an estimate of the actual time, t, required to appraoch equilibrium). As an example, consider the calculations corresponding to Fig. 5 *d*; $1/k_r' = 2$, and hence one would expect the dynamic curves to stop changing when t' is of order 2. This is precisely what is seen in Fig. 5 *d*. A similar effect is seen in the other panels. If dissociation is driven, say, by shearing at a high rate, so

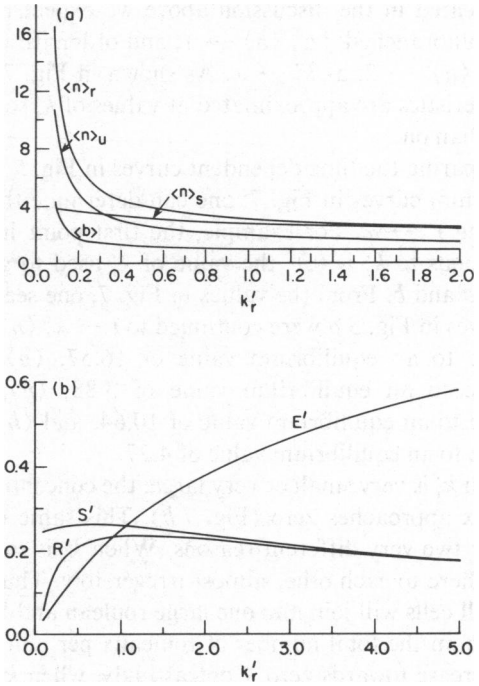

FIGURE 7 Dependence of the equilibrium concentration of rouleaux on the reverse rate constant. (*a*) The equilibrium mean size of a rouleaux, $\langle n \rangle_r$, mean size of a segment, $\langle n \rangle_s$, mean unit size, $\langle n \rangle_u$, and mean number of branches per rouleau, $\langle b \rangle$ vs. the nondimensional reverse rate constant $k_r' = k_r/k_{cc}a_cE_0$. (*b*) The nondimensional equilibrium concentrations of erythrocytes, $E' = E/E_0$, total rouleaux, $R' = R/E_0$ and total straight segments, $S' = S/E_0$ vs. k_r'. In both *a* and *b* the hematocrit is 1% and $k_w' = k_w w/k_{cc}a_c = 0.1$.

that $1/k_r' \ll 1/k_w'$, then $1/k_w'$would provide the appropriate time scale for the establishment of equilibrium.

As time progresses, the dynamic curves stop changing. The time-independent state reached is called an equilibrium state or sometimes a dynamic steady state. In such a state, the rate of growth of rouleaux is exactly balanced by their rate of destruction. If one observes any particular rouleau, it may grow or shrink, but quantities that describe the entire population of rouleaux remain constant.

In Fig. 7 *b* we plot the nondimensional equilibrium concentration of free erythrocytes, E', total rouleaux, R', and total segments, S', vs. k_r' for $k_w' = 0.1$ and $hct = 1$. When k_r' is small, the concentration of free erythrocytes is low, indicating that most erythrocytes are incorporated into rouleaux. In fact, $E' \to 0$ as $k_r' \to 0$, as shown in our previous paper. As k_r' becomes large, erythrocytes dissociate from rouleaux, so $E' \to 1$ as $k_r' \to \infty$. Moreover, as erythrocytes dissociate, rouleaux become progressively smaller. The smallest aggregate considered to be rouleau is a stack of two cells. Because such dimers are a single unbranched segment, $S' = R'$ when all rouleaux are dimers. Notice as k_r' becomes large S' becomes approximately equal to R'.

To further examine the characteristics of the rouleau distribution, we plot in Fig. 7 *a* the equilibrium values of $\langle n \rangle_r$, $\langle n \rangle_s$, and $\langle b \rangle$ vs. k_r' starting with a value of $k_r' = 0.1$. As indicated in the discussion above we expect rouleaux will be unbranched, i.e., $\langle b \rangle \to 1$, and of length two, i.e., $\langle n \rangle_r = \langle n \rangle_s \to 2$, as $k_r' \to \infty$. As shown in Fig. 7 *b* these characteristics are approximated at values of k_r' somewhat larger than one.

Comparing the time dependent curves in Fig. 5 with the equilibrium curves in Fig. 7, one can determine the effect of letting $t' \to \infty$. For example, the first point in Fig. 7 corresponds to $k_r' = 0.1$, the value of k_r' used to generate Figs. 5 *a* and *b*. From the values in Fig. 7, one sees that if the curves in Fig. 5 *a* were continued to $t \to \infty$, $\langle n \rangle_r$ would increase to an equilibrium value of 16.57, $\langle n \rangle_s$ would decrease to an equilibrium value of 3.88, $\langle n \rangle_u$ would increase to an equilibrium value of 10.64, and $\langle b \rangle$ would increase to an equilibrium value of 4.27.

When k_r' is very small or very large, the concentration of rouleaux approaches zero (Fig. 7 *b*). This same effect is seen for two very different reasons. When k_r' is small, red cells adhere to each other almost irreversibly. Thus, eventually all cells will join into one large rouleau and hence at equilibrium the total number of rouleaux per unit volume will decrease towards zero. Contrastingly, when k_r' is very large, red cells adhere to one another very poorly and hence at equilibrium red cell aggregates simply will not occur.

In experimental systems one can vary k_r in two ways. First, if the adhesion of red cells is mediated by macromolecules added to system, e.g., dextran, one can by varying the concentration of the macromolecule vary the adhesive energy holding red cells together (Chien, 1981). Second, if one shears the system at a high rate, aggregates will be pulled apart increasing the value of k_r. Developing a theory that provides a quantitative correspondence between the macromolecular concentration, the shear rate and k_r is an intriguing theoretical problem that is outside the scope of this paper. The work of Bell (1978, 1979, 1981), Capo et al. (1982), and Bell et al. (1984) is relevant in this regard.

The branching parameter, k_w', is also important in determining rouleau sizes and shapes. Although the full sequence of curves shown in Fig. 5 can be repeated for different values of k_w', for brevity we provide in Fig. 8 only data on equilibrium values. In Fig. 8 *a* we plot the equilibrium values of $\langle n \rangle_r$, $\langle n \rangle_s$, and $\langle b \rangle$ vs. $k_w'$for $k_r' = 0.1$ and $hct = 1$. Notice when $k_w' = 0$, $\langle b \rangle = 1$ and all rouleaux are straight segments. As k_w' increases, not only do rouleaux get more branched, but they also get larger. The reason for this is shown in Fig. 8 *b*. With increasing, k_w', cap-wall adhesions between rouleaux are stronger. (To see this, write

$$k_w' = \frac{k_w w E_0}{k_r} \Big/ \frac{k_c a_c E_0}{k_r}$$

as the ratio of cap-wall to cap-cap equilibrium constants.) As rouleaux become larger, the equilibrium concentration of rouleaux must decrease, hence R' decreases with increasing k_w'. Because reactions are reversible, straight segments can breakup. Thus as the cap-wall reaction rate becomes large compared with the cap-cap reaction rate, straight segments dissociate, becoming smaller, and add on to rouleaux as extra branches. Thus, in Fig. 8 *a* $\langle n \rangle_s$

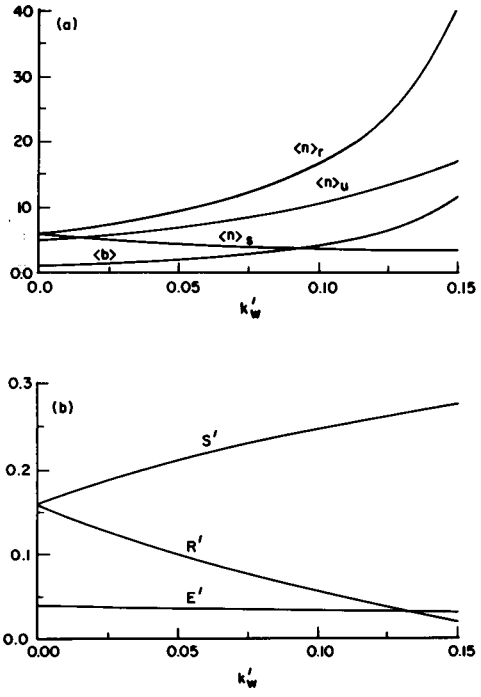

FIGURE 8 Dependence of the equilibrium concentration of rouleaux on the nondimensional cap-wall rate constant, k_w', with $k_r' = 0.1$ and $hct = 1$. The variables plotted are defined in the caption to Fig. 7.

decreases with increasing k'_w and in Fig. 8 *b*, S', the nondimensional concentration of segments increases with k'_w.

The last parameter that affects the equilibrium rouleau distribution is the hematocrit. According to our choice of nondimensional variables (Eq. 46) the hematocrit, through E_0, affects k'_r but not k'_w. Because k'_r is proportional to k_r/E_0, doubling the hematocrit is equivalent to halving k'_r. Thus we need not explicitly study the effects of changing the hematocrit. From Fig. 7 *a* one sees that by increasing the hematocrit, i.e., decreasing k'_r, the mean size of an aggregate increases as one would expect intuitively. However, from Fig. 7 it is difficult to see the full range of effects of changing the hematocrit. In Fig. 9 we show how the various mean quantities describing rouleau size and shape change with *hct*. The parameters for this figure were chosen such that *hct* = 45 corresponds to $k'_r = 0.1$. In *a* where $k'_w = 0.1$, note that $\langle n\rangle_r$, $\langle n\rangle_u$, $\langle n\rangle_s$, and $\langle b\rangle$ all increase monotonically with the hematocrit, although the mean segment size remains small even when *hct* = 45. For the given value of k'_w, rouleaux get larger by increasing the number of branches rather than the size of each branch. However, if k'_w is made smaller (Fig. 9 *b*), then rouleaux get larger by increasing the size of each branch.

Segment Size Distribution

Our theory, via Eqs. 29–31 provides the complete distribution of segment sizes. In Fig. 10 we plot the nondimensional equilibrium segment size distribution $S'(n, c)$ and the nondimensional equilibrium segment weight distribution $nS'(n, c)$ for $k'_r = k'_w = 0.1$ and *hct* = 1. The distribution has several notable characteristics. First, $S'(n, c)$ for $c = 0$, 1, or 2 is a strictly decreasing function of n. So short segments always outnumber long segments. Second, for any given value of n, $S'(n,0)$, $S'(n,1)$, and $S'(n,2)$ are proportional to each other with constants of proportionality that are independent of n. Thus the three distribution curves change in concert. From Eq. 32a the same argument applies to $S'_T(n)$ for $n \geq 2$. Third, the weight distribution curves, $nS(n,c)$, $c = 0$, 1 and 2, and $nS_T(n)$, all have a maximum at the same value of n, $n \simeq -1/\ell n p$. This result can be derived by treating n as a continuous variable, observing that $nS(n,c)$ is proportional np^{n-1} and noting that the derivative of np^{n-1} with respect to n is zero when $n = -1/\ell n\, p$. In Fig. 10 *b* the common maximum is at $n = 2$. For the specified parameters $p = 0.5673$, and our theory predicts $n \simeq 1.76$. Fourth, for these parameter values the concentration of small segments is much higher than the concentration of large segments, with the most prevalent segment being of length two. From Fig. 7 *a* one can see that the mean segment size is approximately four. Thus the mean and the most probable segment lengths are not the same; the mean being larger is

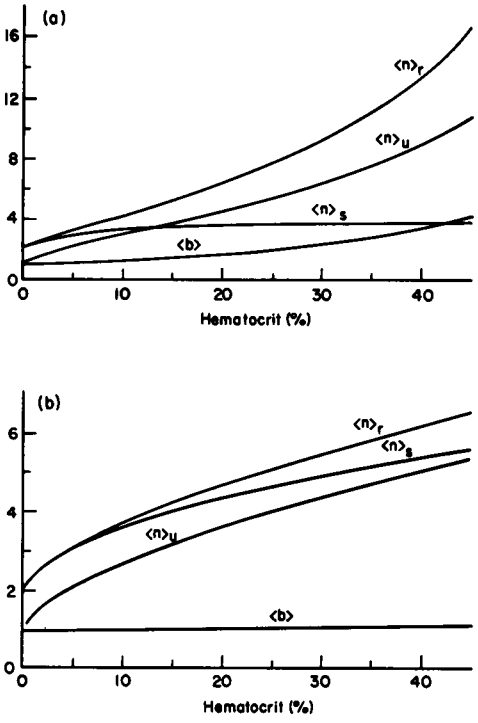

FIGURE 9 Dependence of the equilibrium concentration of rouleaux on the hematocrit, with $k'_r = 0.1$. (*a*) $k'_w = 0.1$, (*b*) $k'_w = 0.01$. The variables plotted are defined in the caption to Fig. 7 *a*.

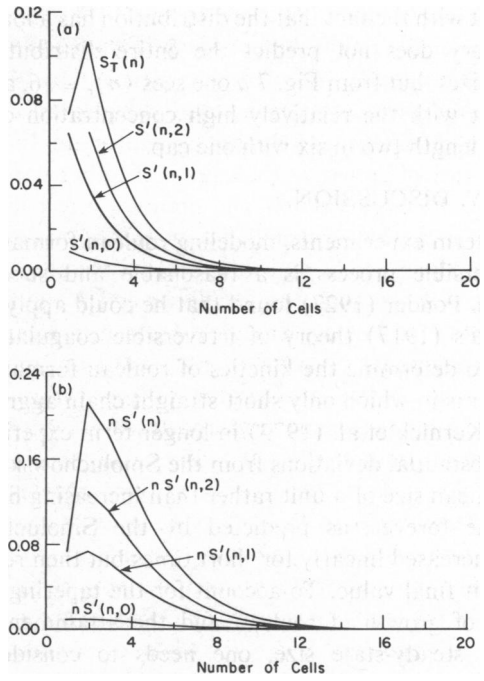

FIGURE 10 The equilibrium size distribution of straight chain segments within rouleaux at 1% hematocrit with $k'_r = k'_w = 0.1$. (*a*) The nondimensional equilibrium concentration of segments of length n and containing c caps, $S'(n,c) = S(n,c)/E_0$ vs. n for $c = 0$, 1, and 2. Also plotted is the total equilibrium concentration of segments of length n, $S'_T(n)$. (*b*) The nondimensional equilibrium segment weight distribution. The nondimensional concentration of red cells in segments of size n with c caps, $nS'(n,c)$, is plotted vs. n. Also plotted is the total nondimensional equilibrium concentration of red cells in segments of length n, $nS'_T(n)$, vs. n.

consistent with the fact that the distribution has a long tail. Our theory does not predict the entire distribution of rouleau sizes, but from Fig. 7 *a* one sees $\langle n \rangle_r \simeq 16$, a value consistent with the relatively high concentration of segments of length two to six with one cap.

V. DISCUSSION

In short term experiments, modeling rouleau formation as an irreversible process is a reasonable and successful approach. Ponder (1927) found that he could apply Smoluchowski's (1917) theory of irreversible coagulation of colloids to determine the kinetics of rouleau formation in experiments in which only short straight chain aggregates formed. Kernick et al. (1973) in longer term experiments found substantial deviations from the Smoluchowski theory. The mean size of a unit rather than increasing linearly with time forever, as predicted by the Smoluchowski theory, increased linearly for short times but then reached a constant final value. To account for the tapering off in the rate of growth of rouleau and the attainment of a constant, steady-state size, one needs to consider the process of rouleau breakup. Rouleaux may dissociate either due to the presence of externally applied forces, such as shearing stresses, or due to the thermodynamic fact that the chemical bonds involved in the macromolecular bridges holding together the erythrocytes within a rouleau eventually break. As a practical matter, under conditions in which cell-cell interactions are sufficiently strong to produce rouleaux, spontaneous disaggregation is rarely, if ever, observed.

Determining as a function of time the sizes and shapes of rouleau that develop under conditions of isotropic, random collisions, is the general kinetic problem of rouleau formation that we began studying in Samsel and Perelson (1982). Here we have extended our original analysis so as to take into consideration the fact that rouleau may break apart. Using the law of mass action, we have generated a set of reversible kinetic equations, that describe changes in R, the total concentration of rouleaux, changes in $S(n,c)$, the concentration of straight chain segments within rouleau that are composed of n cells and have $c = 0, 1, 2$ free ends (caps), and changes in various mean quantities that describe rouleau size and shape. However, unlike our formulation of irreversible kinetics, we have not been able to describe the changes in the concentration of rouleaux with n cells and c caps under the assumption of reversible reactions, the problem being that one can not uniquely describe the products that form when a rouleau with n cells and c caps dissociate.

Besides providing a more accurate description of the kinetics of rouleau formation, the incorporation of dissociation processes has allowed us to use the principle of detailed balance to ascertain constraints on the rate constants, describing chain elongation and branching, that were not apparent on our earlier models involving only irreversible reactions.

Mass-action models of rouleau formation naturally lead to the formation of models containing infinite systems of ordinary differential equations. Here the equations describe the growth and breakup of segments containing n cells and c caps, $n = 1, 2, \ldots$. We have shown that if the faces of all red cells are equally reactive, irrespective of the size and shape of the aggregate in which they are found, and if aggregates do not form rings or loops, then the resulting sets of differential equations that model the kinetics of aggregation can be solved by using a modification of the Flory-Stockmayer method from polymer chemistry. Using this technique, the size distribution of branches, $S(n,c)$, is found as a function of two variables: p_f, the probability that an erythrocyte face (i.e., a reactive site) is free, and p_w, the probability that an erythrocyte face is bound to the wall of a rouleau. The two variables, p_f and p_w, change according to a pair of nonlinear differential equations, Eq. 44. Solving these equations and substituting into the Flory-Stockmayer expressions for $S(n,c)$ then provides a solution to the infinite system of ordinary differential equations that describe the kinetics of rouleau formation.

Examining both the kinetic and equilibrium solutions of our mass-action model allows us to reach some tentative conclusions about the rate constants that describe the kinetic process. If k'_r, the nondimensional reverse rate constant defined by Eq. 46, is larger than one, then dissociation occurs very frequently compared with chain elongation, either via cap-cap or cap-erythrocyte reactions, and rouleaux tend to be very small. We feel that values of k'_r of order of 0.1 are probably typical of experiments done at low hematocrit with fibrinogen as the bridging macromolecule in which rouleaux with a mean unit size of order eight are seen (Chien et al., 1967). When dextran is used as the bridging macromolecule, rouleaux tend to be even smaller, with $\langle n \rangle_u \simeq 3$ (Jan and Chien, 1973), and hence k'_r would need to be larger, say $k'_r \simeq 0.5$, to fit the experimental data. The second variable we have studied is k'_w, the nondimensional forward rate constant governing branching reactions (cap wall or erythrocyte wall). If k'_w is much less than 0.1, then very little branching occurs, and, at least with $k'_r \geqq 0.1$, rouleaux tend to be small straight chains. As k'_w is increased, for a fixed value of k'_r, rouleaux tend to become larger and more branched. A value of k'_w of order 0.1 might be typical of the experiments of Jan and Chien (1973). In fitting the data of Kernick et al. (1973), we used $k'_w = 0.2$ with $k'_r = 0.4$.

Our theory of rouleau formation does not explicitly place bounds on acceptable values of the rate constants. Consequently, one can examine parameter values that correspond to unphysical situations. We were thus able to discover a failure of our model, which is both instructive and interesting. If the rate of branching is too high and the reverse rate constant is too low, then it is possible to compute solutions where the concentration of rouleaux becomes negative (see Fig. 11). The reason is simple: if the

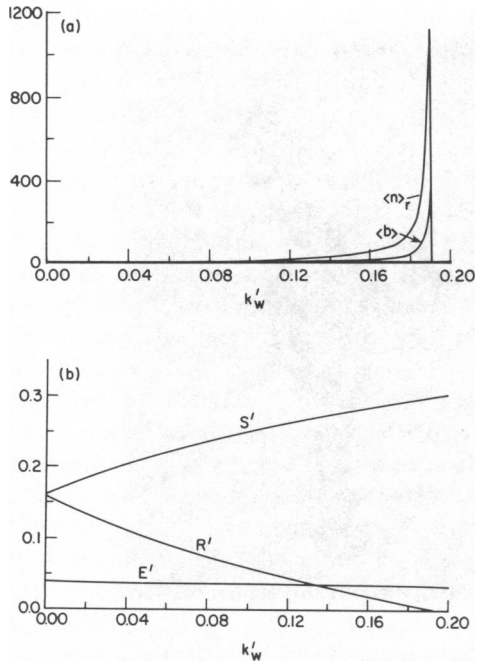

FIGURE 11 Demonstration of model failure at high values of the branching rate. Plotted are the equilibrium values of quantities that describe rouleau size and shape as detailed in the caption to Fig. 7, vs. k'_w for $k'_r = 0.1$. Note in *a* that $\langle n \rangle_r$ and $\langle b \rangle \rightarrow \infty$ as $R' \rightarrow 0$ in *b*.

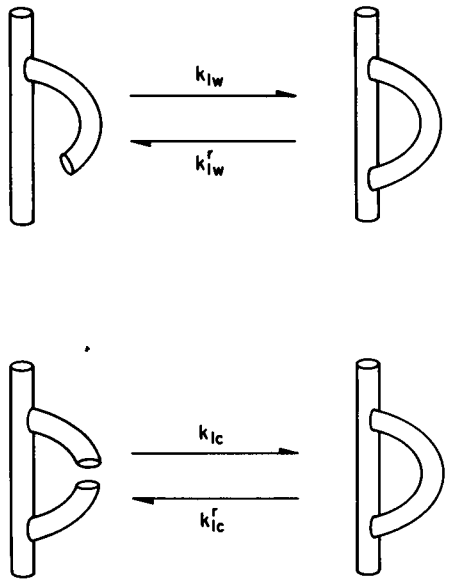

FIGURE 12 A loop can be formed by one of two processes: (*a*) a cap can adhere to the wall of the rouleau of which it is part, or (*b*) two caps on the same rouleau can join. These reactions are assumed to be reversible with rate constants $k_{\ell w}$, $k^r_{\ell w}$, $k_{\ell c}$, and $k^r_{\ell c}$ as indicated.

total concentration of caps, M, is positive, the model predicts that cap-cap or cap-wall adhesions occur, thus reducing the number of free rouleaux. With insufficient dissociation, most cells become bound in a single aggregate with many caps and many branches. But since $M > 0$, our model predicts that even when there is a single aggregate, R will continue to decrease and become negative. This can be seen in Eq. 16. As E and R approach zero, the negative terms dominate and $dR/dt < 0$. Further, one finds by solving the algebraic problem for the equilibrium concentrations, that the equilibrium concentration of rouleaux can be negative.

The heart of the problem is the assumption that rouleaux are topologically trees, and thus have no loops. In fact, rouleaux do form loops, as can easily be verified by direct observation (see Fig. 13). Thus, a model of rouleau formation that is to be valid for long times and for all possible parameter values must include loop formation. Methods for modeling loop formation are under development and will be discussed in a future publication. For our purposes here, it sufficies to show that including loop formation in our model will prevent R from going negative. However, we expect that in situations in which k'_w is not large and in which R remains positive, rouleau formation can be modeled accurately without considering loop formation.

Loops can form at least by two mechanisms: two caps on the same rouleau can join or a cap can join to the wall of the rouleau of which it is part (see Fig. 12). Let k_{lc} and k_{lw} denote the forward rate constants per unit area for these loop generating processes. The average number of caps per rouleau is M/R. If this number is large and the branches of the rouleau are sufficiently flexible that one can assume a uniform density of caps within a rouleau, the law of mass action provides that the rate at which caps collide is proportional to $(M/R)^2$. Because such collisions occur in all R rouleaux per unit volume, one can assume that the net rate of loop formation by cap-cap reactions is $k_{lc}a_cR(M/R)^2$. One cap disappears in each cap-cap reaction and thus this term would have to be subtracted from the dM/dt equation, Eq. 12. Note that as $R \rightarrow 0$, this term approaches infinity and hence dM/dt will go negative, forcing M to approach zero. (When $M = 0$, this term is zero and hence M will not go negative). By an analagous argument, one can assume cap-wall reactions lead to loop formation at a mean rate proportional to $k_{lw}R(W/R)(M/R)$. Because a cap also disappears in each cap-wall reaction, this term is also subtracted from Eq. 12 and hence contributes to dM/dt going negative as $R \rightarrow 0$. As the final step in our argument, note from Eq. 16 that if $M \rightarrow 0$ as $R \rightarrow 0$, then dR/dt remains positive and R will remain positive. Although this model for ring closure is probably too simple to be accurate, it does illustrate the general principle, in the presence of ring closure reactions the concentration of caps will be sufficiently reduced that all the variables in our model will remain positive. Other, more refined, models of ring closure and ring opening and predictions about the geometry of the resulting aggregate will be presented in a later paper.

One additional feature of rouleau formation that is not accounted for in our model is the possibility of wall-wall interactions. Such interactions can occur when two rou-

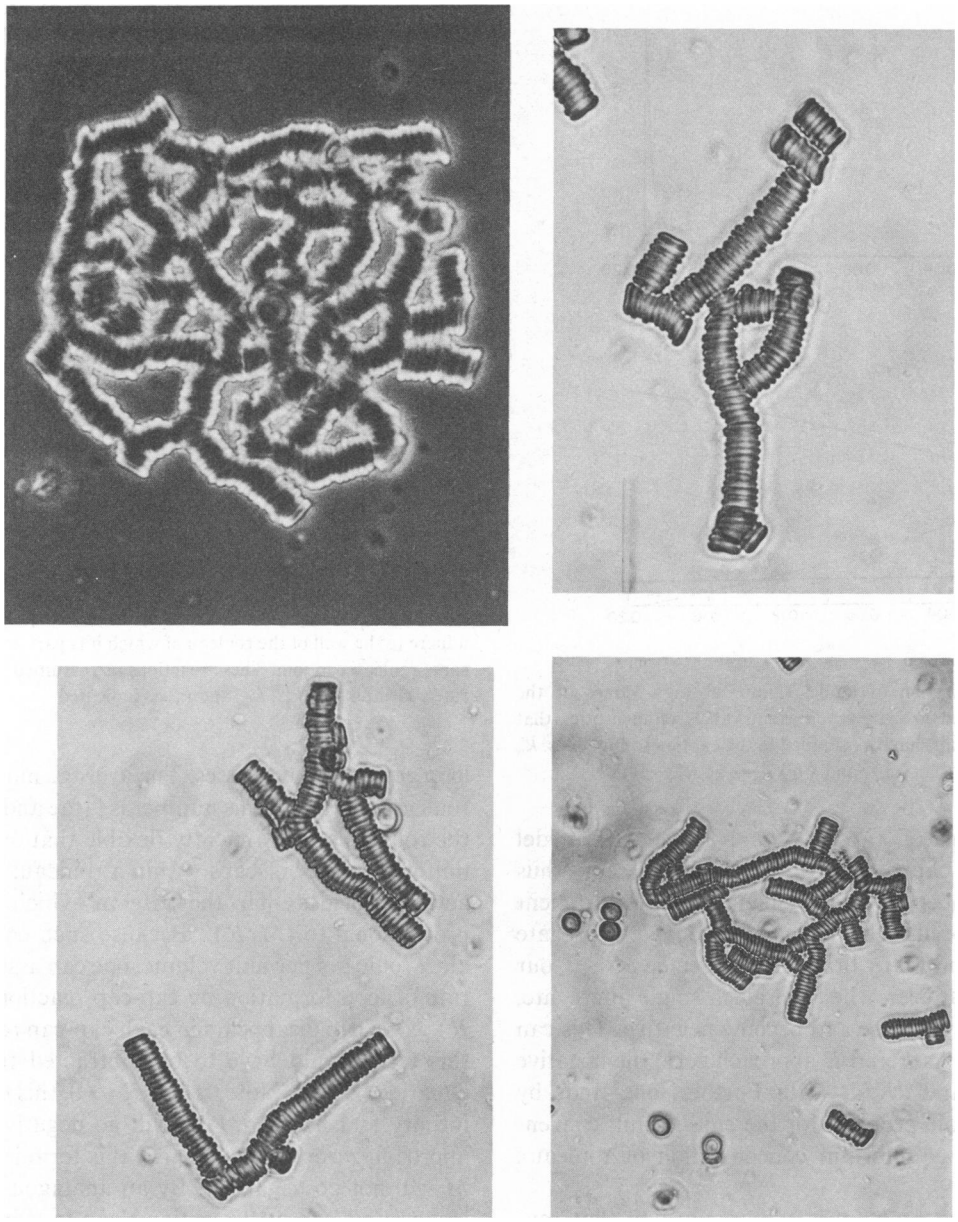

FIGURE 13 Rouleaux exhibiting loops and wall-wall interactions. (*a*) End stage of a reaction in which most caps have disappeared by having participated in loop forming reactions. (*b*) A wall-wall interaction that probably was generated by the collision of two rouleaux. (*c*) A wall-wall interaction that probably was generated in a loop forming reaction. (*d*) A large rouleaux exhibiting multiple loops and wall-wall interactions.

leaux collide or when a loop within a rouleau forms (see Fig. 13 *b*,*c*). Wall-wall interactions reduce the surface area on a rouleau available for reaction and thus will also contribute to preventing R from going negative. The importance of wall-wall interactions is hard to assess and is a subject for future research.

Our general view of rouleau formation is that the process can be decomposed into a number of stages. First, erythrocytes join to each other and existing straight stacks to form cylindrical rouleaux. After the stacks become sufficiently large, some erythrocytes stick to the wall of the rouleau and form branches. We showed in our previous paper that these reactions can be modeled as irreversible, addition reactions. As erythrocytes are depleted, condensation reactions between existing rouleau become the dominant process and lead to the formation of large aggregates. Dissociation reactions become significant as large aggregates form, both because shear forces generate increasing torques and because spontaneous dissociation of erythrocytes, even if extremely unlikely for two cells, becomes more and more likely as the number of adhesive interfaces increase. If dissociation reactions are very unlikely, or if branching and elongation reactions very likely, rouleaux will continue to condense until there is only one or a few

large aggregates. At this stage, loop formation (which could occur at any point in the reaction) must become the dominant reaction, free erythrocytes and other rouleaux are simply unavailable for reaction. In principle, the rouleau could continue to fold back on itself until there were no longer any free ends. An example of a rouleau approaching this state is shown in Fig. 13 *a*.

At least three different experimental approaches can be used to test our theory. First, optical measurements of red cell suspensions can be used to provide estimates of the degree of aggregation under controlled shear conditions (cf., Schmid-Schönbein et al., 1972; Usami and Chien, 1973; Mills et al., 1980*a*, *b*). However, to determine from data quantitative information about the mean rouleau size requires the use of a physical model (e.g., assuming the rouleau is an unbranched cylinder), and therefore the method itself is subject to verification by some more direct measurement.

Second, low speed flow cytometry can be used to measure the size distribution of aggregates (Eisert et al., 1981); conventional high speed flow cytometry involves shear rates that disaggregate essentially all rouleaux (Samsel and Perelson, unpublished observations). This technique has the drawback that the shear rate in the entrance flow regime is difficult to control and make uniform, and only small aggregates can be accurately measured.

Finally, direct observation of rouleaux, stationary or in flow, is possible. Contrarotatory or conventional cone-plate or Couette viscometers, as well as simpler flow chambers, can allow direct observation of aggregation of red cells in constant shear fields. High resolution optics and rapid recording devices are necessary, and to our knowledge such measurements are technically difficult and have not been made. However, the technology is available to make such measurements and to accurately test our theory.

APPENDIX

Reverse Reactions

Here we derive the detailed equations describing the time rate of change of $S(n, c)$ when cell-cell interactions are assumed to be reversible. The one cell and two cell segments, $S(1, 1)$ and $S(2, 2)$ must be treated specially. The forward reaction terms derived in our previous paper (Samsel and Perelson, 1982) remain the same and we only add the contributions of the reverse reactions. An $S(n, 0)$ with $n > 2$ can split to form $S(1, 1)$ in two ways, $S(2, 0)$ can only split in one way, but forms two $S(1, 1)$. Hence the contribution from the breakup of $S(n, 0)$ for $n > 1$ to the growth of $S(1, 1)$ is $2k^r_{cc}S(n, 0)$. Similarly, any $S(n, 1)$, where $n > 2$ can break up in only one way to form a one-cell one-cap branch. Some of these reactions are illustrated in Fig. 14. Summing all the contributions to $S(1, 1)$ growth we find

$$\begin{aligned} dS(1,1)/dt = {} & k_{cw}EW - k_{cc}a_cES(1,1) \\ & - k_{cc}a_cMS(1,1) - k_{cw}WS(1,1) \\ & + k^r_{cc}S(2,1) - k^r_{cw}S(1,1) + 2k^r_{cw}S(1,0) \\ & + k^r_{cc}\sum_{c=0}^{1}\sum_{n=c+2}^{\infty}(2-c)S(n,c). \end{aligned} \tag{A1}$$

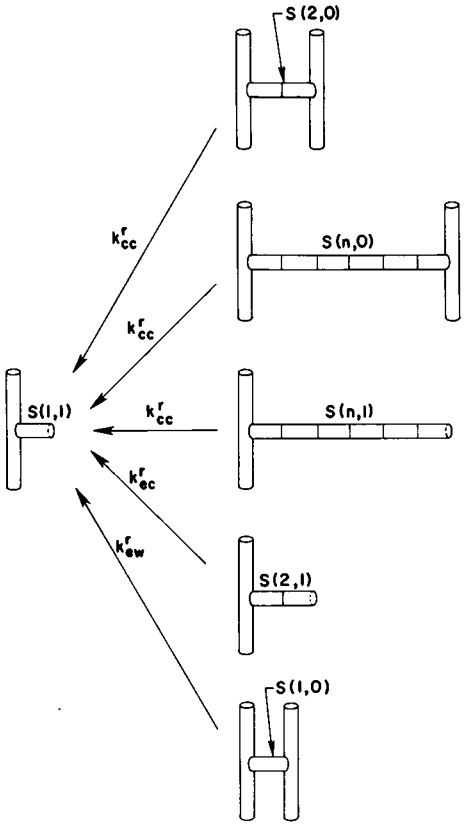

FIGURE 14 Diagrammatic representation of some of the reverse reactions that lead to the formation of $S(1,1)$, branches that contain one cell and one cap.

By similar reasoning, one may write an equation for $dS(2, 2)/dt$, adding the new reverse terms to the forward terms already given in Eq. I.A1.2. Breakup of $S(n, 2)$ for $n > 2$ can produce new $S(2, 2)$ in two ways or when $n = 4$ two $S(2, 2)$. By cap-wall or cap-cap dissociation $S(n, 1)$ can produce $S(2, 2)$ in only one way. Thus we find

$$\begin{aligned} dS(2,2)/dt = {} & \frac{1}{2}k_{cc}a_cE^2 - 2k_{cc}a_cES(2,2) \\ & - 2k_{cc}a_cS(2,2)M - 2k_{cw}S(2,2)W \\ & - k^r_{cc}S(2,2) + 2k^r_{cc}S(3,2) + k^r_{cw}S(2,1) \\ & + k^r_{cc}\sum_{c=1}^{2}\sum_{n=c+2}^{\infty}cS(n,c), \end{aligned} \tag{A2}$$

The equation for $S(n, 0)$ is particularly simple, since branches with zero caps cannot be formed by the breakup of other branches. A branch with n cells has $n - 1$ junctions between cells, each of these a potential breakpoint. The rate of cap-cap breakup is consequently proportional to $(n - 1)S(n, 0)$. Additionally, a branch with no caps has two branch points where a cap may detach from a wall. Incorporating these reverse reaction terms into Eq. I.A1.3, we find

$$\begin{aligned} dS(n,0)/dt = {} & k_{cw}WS(n,1) \\ & + \frac{1}{2}k_{cc}a_c\sum_{k=1}^{n-1}S(k,1)S(n-k,1) \\ & - k^r_{cc}(n-1)S(n,0) - 2k^r_{cw}S(n,0). \end{aligned} \tag{A3}$$

The simplicity of this expression is lost when $S(n, 1)$ is considered. Shortening of caps adds both positive and negative terms to the equation

for $S(n, 1)$. Similarly, $S(n, 1)$ is formed by breakup of $S(n, 0)$ and lost by their own breakup. Thus we have for $n > 1$

$$\begin{aligned} dS(n,1)/dt = {} & k_{cc}a_c E[S(n-1,1) - S(n,1)] \\ & + 2k_{cc}a_c \sum_{k=2}^{n-1} S(k,2)S(n-k,1) \\ & - k_{cc}a_c MS(n,1) + k_{cw}W[2S(n,2) - S(n,1)] \\ & + k^r_{cc}[S(n+1,1) - S(n,1)] \\ & + k^r_{cc} \sum_{m=n+2}^{\infty} S(m,1) + 2k^r_{cc} \sum_{m=n+1}^{\infty} S(m,0) \\ & - k^r_{cc}(n-2)S(n,1) \\ & + k^r_{cc}[2S(n,0) - S(n,1)]. \end{aligned} \tag{A4}$$

Finally, we can write the equation for $dS(n, 2)/dt$, including reversible terms. We find, for $n > 2$,

$$\begin{aligned} dS(n,2)/dt = {} & 2k_{cc}a_c E[S(n-1,2) - S(n,2)] \\ & + 2k_{cc}a_c \sum_{k=2}^{n-2} S(k,2)S(n-k,2) \\ & - 2k_{cc}a_c S(n,2)M - 2k_{cw}WS(n,2) \\ & + 2k^r_{cc}[S(n+1,2) - S(n,2)] \\ & + k^r_{cc} \sum_{m=n+1}^{\infty} S(m,1) + 2k^r_{cc} \sum_{m=n+2}^{\infty} S(m,2) \\ & - k^r_{cc}(n-3)S(n,2) + k^r_{cw}S(n,1). \end{aligned} \tag{A5}$$

It is also useful to derive equations for $S(0)$, $S(1)$, and $S(2)$ defined by

$$S(0) \equiv \sum_{n=1}^{\infty} S(n, 0) \tag{I.67}$$

$$S(1) \equiv \sum_{n=1}^{\infty} S(n, 1)\,, \tag{I.68}$$

$$S(2) \equiv \sum_{n=2}^{\infty} S(n, 2)\,. \tag{I.69}$$

Although differential equations for these variables do not form a closed system, their derivation provides a useful step in recovering equations for dS/dt (Eq. 15) and dR/dt (Eq. 16) from the detailed system given above.

Summing Eq. A3 over n gives

$$\begin{aligned} dS(0)/dt = {} & \frac{1}{2}k_{cc}a_c S(1)^2 + k_{cw}WS(1) \\ & - k^r_{cc}[N(0) - S(0)] - 2k^r_{cw}S(0), \end{aligned} \tag{A6}$$

where we have denoted the concentration of cells belonging to $S(n, c)$ by $N(c)$, i.e..

$$N(c) = \sum_{n=1}^{\infty} nS(n, c)\,, \qquad c = 0, 1, 2\,. \tag{A7}$$

Similarly, summing Eq. A1 and Eq. A4 over n gives

$$\begin{aligned} dS(1)/dt = {} & k_{cw}EW + 2k_{cc}a_c S(1)S(2) \\ & - k_{cc}a_c MS(1) + k_{cw}W[2S(2) - S(1)] \\ & + 2k^r_{cc}N(0) - k^r_{cw}S(1) \\ & + 2(k^r_{cw} - k^r_{cc})S(0) \\ & + (k^r_{cw} - k^r_{cw})S(1,1). \end{aligned} \tag{A8}$$

Finally, summing equations A2 and A5 gives

$$\begin{aligned} dS(2)/dt = {} & \frac{1}{2}k_{ee}a_e E^2 + 2k_{cc}a_c S(2)^2 \\ & - 2k_{cc}a_c MS(2) - 2k_{cw}WS(2) \\ & + k^r_{cc}[N(1) + N(2)] \\ & - (2k^r_{cc} - k^r_{cw})S(1) - 3k^r_{cc}S(2) \\ & + (k^r_{cc} - k^r_{cw})S(1,1) \\ & + (k^r_{cc} - k^r_{ce})S(2,2). \end{aligned} \tag{A9}$$

If all the reverse rate constants are assumed equal (Eq. 10), we have

$$\begin{aligned} dS(0)/dt = {} & \frac{1}{2}k_{cc}a_c S(1)^2 + k_{cw}WS(1) \\ & - k_r N(0) - k_r S(0), \end{aligned} \tag{A10}$$

$$\begin{aligned} dS(1)/dt = {} & k_{cw}EW + 2k_{cc}a_c S(1)S(2) \\ & - k_{cc}a_c MS(1) + k_{cw}W[2S(2) - S(1)] \\ & + 2k_r N(0) - k_r S(1), \end{aligned} \tag{A11}$$

and

$$\begin{aligned} dS(2)/dt = {} & \frac{1}{2}k_{ee}a_e E^2 + 2k_{cc}a_c S(2)^2 \\ & - 2k_{cc}a_c MS(2) - 2k_{cw}WS(2) \\ & + k_r[N(1) + N(2)] \\ & - 3k_r S(2) - k_r S(1). \end{aligned} \tag{A12}$$

Eq. 15 for dS/dt can now be derived by summing Eqs. A10–A12 and noting that the total number of cells bound in rouleaux, $E_0 - E$, is equal to $N(0) + N(1) + N(2)$.

A direct derivation of dR/dt is also possible. Breakup of any large rouleau will usually create two smaller rouleaux. In a rouleau with n cells, there are $n - 1$ bonds holding the cells together. If a single cell is lost from a cap, then no new rouleaux are created. Thus, there are $n - c - 1$ sites in a rouleau with c caps and n cells where breakage will result in the formation of two rouleaux from one rouleau. Hence, if we assume that all reverse rate constants are equal, the contribution to dR/dt from the reverse reactions is found to be

$$k_r \sum_{n,c} (n - c - 1)R(n, c)\,. \tag{A13}$$

As usual, this term requires careful consideration for the lowest values of n and c. When $n = c = 2$, breakup results in the loss of rouleaux only, since single cells are produced. This is taken into account by the summation, which counts the contribution from $R(2, 2)$ to be $-k_r R(2, 2)$. Similarly, $R(3, 2)$ conserves rouleaux by its breakage and does not contribute to the equation. The summation in Eq. A7 is easily evaluated, giving the final result

$$\begin{aligned} dR/dt = {} & \frac{1}{2}k_{ee}a_e E^2 - \frac{1}{2}k_{cc}a_c M^2 \\ & - k_{cw}MW + k_r(E_0 - E - M - R)\,. \end{aligned} \tag{A14}$$

We would like to thank Dr. Richard Skalak for stimulating and encouraging discussions and Dr. George Bell for his helpful criticism. We dedicate this work to Aharon Katchalsky-Katzir, a pioneer of the macromolecular bridging hypothesis, whose spirit lives on despite his death at the hands of terrorists.

This work was initiated while Dr. A. S. Perelson was in the Division of Biology and Medicine, Brown University, and was supported by BRSG grant S07 RR05664-11, awarded by the Biomedical Research Support Grant Program, Division of Research Resources, The National Institutes of Health. Later parts of this work were performed under the auspices of the U. S. Department of Energy. Dr. Perelson is the recipient of an National Institutes of Health Research Career Development Award 5 K04 AI00450-04.

Received for publication 5 April 1983 and in final form 16 September 1983.

REFERENCES

Adler, P. M. 1979. A study of disaggregation effects in sedimentation. *AICHE J.* 25:487–493.

Bak, T. A. 1963. Contributions to the Theory of Chemical Kinetics. W. A. Benjamin, Inc., New York. 34–38.

Bell, G. I. 1978. Models for the specific adhesion of cells to cells. *Science (Wash. DC).* 200:618–627.

Bell, G. I. 1979. A theoretical model for adhesion between cells mediated by multivalent ligands. *Cell Biophys.* 1:133–147.

Bell, G. I. 1981. Estimate of the sticking probability for cells in uniform shear flow with adhesion caused by specific bonds. *Cell Biophys.* 3:289–304.

Bell, G. I., M. Dembo, and P. Bongrand. 1984. Cell-cell adhesion: competitions between nonspecific repulsion and specific bonding. *Biophys. J.* In press.

Brooks, D. E., and G. V. F. Seaman. 1973. The effect of neutral polymers on the electrokinetic potential of cells and other charged particles. I. Models for the zeta potential increase. *J. Colloid Interface Sci.* 43:670–686.

Brooks, D. E. 1973*a*. The effect of neutral polymers on the electrokinetic potential of cells and other charged particles. II. A model for the effect of adsorbed polymer on the diffuse double layer. *J. Colloid Interface Sci.* 43:687–699.

Brooks, D. E. 1973*b*. The effect of neutral polymers on the electrokinetic potential of cells and other charged particles. III. Experimental studies on the dextran/erythrocyte system. *J. Colloid Interface Sci.* 43:700–713.

Brooks, D. E. 1973*c*. The effect of neutral polymers on the electrokinetic potential of cells and other charged particles. IV. Electrostatic effects in dextran-mediated cellular interactions. *J. Colloid Interface Sci.* 43:714–726.

Capo, C., F. Garrouste, A.-M. Benoliel, P. Bongrand, A. Ryter, and G. I. Bell. 1982. Concanavalin-A-mediated thymocyte agglutination: A model for a quantitative study of cell adhesion. *J. Cell Sci.* 56:21–48.

Chang, H. N., and C. R. Robertson. 1976. Platelet aggregation by laminar shear and Brownian motion. *Ann. Biomed. Eng.* 4:151–183.

Chien, S., S. Usami, R. J. Dellenback, M. I. Gregersen, L. B. Nanninga, and M. M. Guest. 1967. Blood viscosity: influence of erythrocyte aggregation. *Science* (Wash. DC) 157:829–831.

Chien, S. 1975. Biophysical behavior of red cells in suspensions. *In* The Red Blood Cell. D. M. N. Surgenor, editor. Academic Press, Inc., New York. Second ed. 2:1031–1133.

Chien, S. 1976. Electrochemical interactions between erythrocyte surfaces. *Thromb. Res.* 8(Suppl II):189–202.

Chien, S. 1981. Electrochemical interactions and energy balance in red cell aggregation. *In* Topics in Bioelectrochemistry and Bioenergetics, G. Milazzo, editor. Wiley-Interscience, New York. 4:73–131.

DeLisi, C., and A. S. Perelson. 1976. The kinetics of aggregation phenomena. I. Minimal models for patch formation on lymphocyte membranes. *J. Theor. Biol.* 62:159–210.

Dintenfass, L. 1976. Rheology of Blood in Diagnostic and Preventive Medicine. Butterworth, London.

Dintenfass, L. 1979. Aggregation of red cells and blood viscosity under near-zero gravity. *Biorheology.* 16:29–36.

Ehrly, A. M. 1971. Disaggregation of erythrocyte aggregates. *Proc. Europ. Conf. Microcirculation, Aalborg 1970,* 6th Karger, Basel.

Eisert, R. M., G. Eckert, and W. G. Eisert. 1981. Alteration of blood cells and microaggregate formation during storage monitored by laser flow cytometry. *Anal. Quant. Cytology.* 3:309–314.

Evans, C. W., and J. Proctor. 1978. A collision analysis of lymphoid cell aggregation. *J. Cell Sci.* 33:17–36.

Evans, E., and Y.-C. Fung. 1972. Improved measurements of the erythrocyte geometry. *Microvasc. Res.* 4:335–347.

Flory, P. J. 1953. Principles of Polymer Chemistry. Cornell University Press, Ithaca, New York. 317–398.

Goldstone, J., H. Schmid-Schönbein, and R. Wells. 1970. The rheology of red blood cell aggregates. *Microvasc. Res.* 2:273–286.

Jan, K-M., and S. Chien. 1973. Role of surface electric charge in red blood cell interactions. *J. Gen. Physiol.* 61:638–654.

Jones, M. N., and R. Perry. 1979. The kinetics of cellular aggregation induced by turbulent flow. *J. Theoret. Biol.* 81:75–89.

Katchalsky, A., and P. Curran. 1965. Nonequilibrium Thermodynamics in Biophysics. Harvard University Press, Cambridge, MA. 94–97.

Kernick, D., A. W. L. Jay, S. Rowlands, and L. Skibo. 1973. Experiments on rouleau formation. *Can. J. Physiol. Pharmacol.* 51:690–699.

Levich, V. G. 1962. Physiochemical Hydrodynamics. Prentice Hall, Englewood Cliffs, NJ. 207–230.

Lister, J. 1859. XXXI. On the early stages of inflammation. *Philos. Trans. R. Soc. Lond.* 148:645–702.

Miale, J. B. 1977. Laboratory Medicine Hematology. Fifth ed. C. V. Moseby Co., St. Louis, MO.

Mills, P., D. Quemada, and J. Dufaux. 1980*a*. Etude de la cinétique d'aggrégation érythrocytaire dans un écoulement de Couette. *Revue Phys. Appl.* 15:1357–366.

Mills, P., D. Quemada, and J. Dufaux. 1980*b*. An optical method for studying red blood cells orientation and aggregation in a Couette flow of blood suspension. *In* Rheology, Vol. 3, Applications, G. Astarita, G. Manucci, and L. Nicolais, editors. Plenum Press, New York. 567–572.

Perelson, A. S. 1980. Mathematical immunology. *In* Mathematical Models in Molecular and Cellular Biology. L. A. Segel, editor. Cambridge University Press, Cambridge, England. 376–403.

Perelson, A. S., and F. W. Wiegel. 1982. The equilibrium size distribution of rouleaux. *Biophys. J.* 37:515–522.

Ponder, E. 1927. On sedimentation and rouleau formation. II. *Q. J. Exp. Physiol.* 16:173–194.

Richardson, P. D. 1973. Effect of blood flow velocity on growth rate of platelet thrombi. *Nature (Lond.).* 245:103–104.

Saffman, P. G., and J. S. Turner. 1956. On the collision of drops in turbulent clouds. *J. Fluid Mech.* 1:16–30.

Samsel, R. W., and A. S. Perelson. 1982. Kinetics of rouleau formation. I. A mass action approach with geometric features. *Biophys. J.* 37:493–514.

Schmid-Schönbein, H., E. Volger, and H. J. Klose. 1972. Microrheology and light transmission of blood. II. The photometric quantification of red cell aggregate formation and dispersion in flow. *Pfluegers Arch. Eur. J. Physiol.* 333:140–155.

Skalak, R., P. R. Zarda, K.-M. Jan, and S. Chien. 1981. Mechanics of rouleau formation. *Biophys. J.* 35:771–781.

Smoluchowski, M. V. 1917. Versuch einer mathematischen Theorie der Koagulationkinetik Kolloider Lösungen. *Z. Phys. Chem.* 92:129–168.

Stockmayer, W. H. 1943. Theory of molecular size distribution and gel formation in branched-chain polymers. *J. Chem. Phys.* 11:45–55.

Swift, D. L., and S. K. Friedlander. 1964. The coagulation of hydrosols by Brownian motion and laminar shear flow. *J. Colloid Sci.* 19:621–647.

Usami, S., and S. Chien. 1973. Optical reflectometry of red cell aggregation under shear flow. *Bibl. Anat.* 11:91–97.

Usami, S., R. G. King, S. Chien, R. Skalak, C. R. Huang, and A. L. Copley. 1975. Microcinephotographic studies on red cell aggregation in steady and oscillatory shear—a note. *Biorheology.* 12:323–325.

Wiegel, F. W., and A. S. Perelson. 1982. The statistical mechanics of red blood cell aggregation: the distribution of rouleaux in thermal equilibrium. *J. Stat. Phys.* 29:813–848.

Zaiko, M. V., and Y. V. Zarétskaya. 1981. Determination of the rate constants of effective collisions of erythrocyte aggregates in the blood. *Mech. Composite Materials.* 17:360–363.